Triassic chronostratigraphy utilising Magnetostratigraphy:

The De Geerdalen, Snadd, Tschermakfjellet and Botneheia formations in wells 7830/3-u-1, 7831/2-u-1 and 7831/2-u-2, Northern Barents Sea.

Report for the Norwegian Petroleum Directorate

Mark W Hounslow[1], Samuel E Harris[1] & Victoria A Lucas[1], Atle Mørk[2]

[1]Centre for Environmental Magnetism and Palaeomagnetism, Lancaster Environment Centre, Lancaster University, Bailrigg, Lancaster, U.K.

+ 44 1524 510238, m.hounslow@lancaster.ac.uk

[2] SINTEF Petroleum Research, NO-7465, Trondheim, Norway

+47 73 59 11 63 atle.mork@sintef.no

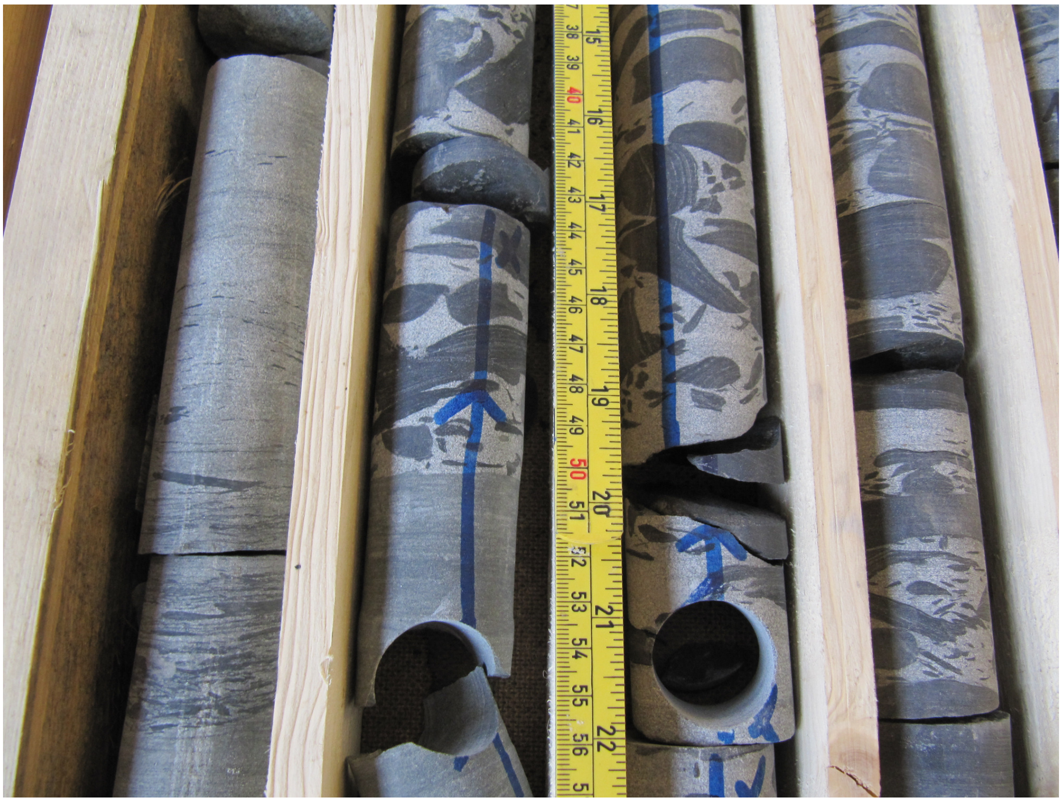

June 2013

Executive Summary

The magnetic polarity data in three NPD wells through the Botneheia Fm, Tschermakfjellet Formation and Snadd Formation south of Kong Karls Land have been evaluated for their magnetostratigraphy, with the aim of understanding the chronostratigraphy of the Ladinian-Carnian units in the northern Barents Sea. The magnetostratigraphy of these wells suggests the boundary between the Botneheia and Tschermakfjellet formations in these wells is within the mid Ladinian (probably mid part of the late Ladinian *Nathorstites mclearni* ammonoid zone, at around a U/Pb age of 238.5 Ma. The boundary between the Tschermakfjellet Formation and the overlying Snadd Formation (De Geerdalen Formation) is close to the upper boundary of the late Ladinian *Nathorstites mclearni* ammonoid zone at around a U/Pb age of 238 Ma. The Ladinian-Carnian boundary (as defined at the Carnian GSSP in Italy) is within the Snadd Formation. These correlations are consistent with the fragmentary ammonoid biostratigraphy from the cores and the bio-magnetostratigraphic data from central Spitsbergen in this same interval.

The petromagnetic and magnetostratigraphic data from the youngest core examined (7830/3-u-1) suggests the Snadd Formation in this well can be divided into three major sediment packages. The lower two being separated by a disconformity, within 3 m of the inferred Ladinian-Carnian boundary. The youngest package, also with a likely disconformable base, has a much larger sedimentation rate than the older two, and in this core extends upwards into the mid to upper parts of the Julian-1 sub-stage (oldest sub-stage in the Carnian). These packages probably relate to the clinoform structures seen in seismic images through the Snadd Formation.

These correlations suggest the Re/Os dates from the same cores analysed here may be too young by some 2 Ma, when compared to the U/Pb dates from zircons. There is probably insufficient ammonoid calibration of the Barents Sea palynological data to violate the high-resolution correlations proposed here, since age equivalents of the *Nathorstites*-bearing beds (i.e. those covering the late Ladinian-earliest Carnian interval) are relatively poorly known in the Barents Sea region.

1 Introduction

1.1 Chronostratigraphy of the Late Triassic in the Svalbard region

The chronostratigraphy for the late Triassic units on Svalbard (the Tschermakfjellet Fm, De Geerdalen Fm and lower part of Wilhelmøya Subgroup) and the northern Barents Sea are very poorly constrained. On Svalbard, ammonoid dated units are restricted to only two intervals, 1) in the lowest part of the Tschermakfjellet Fm (Early Carnian) and 2) in the Slottet Bed (Early Norian) at the base of the Wilhelmøya Subgroup (Dagys & Weitschat 1993).

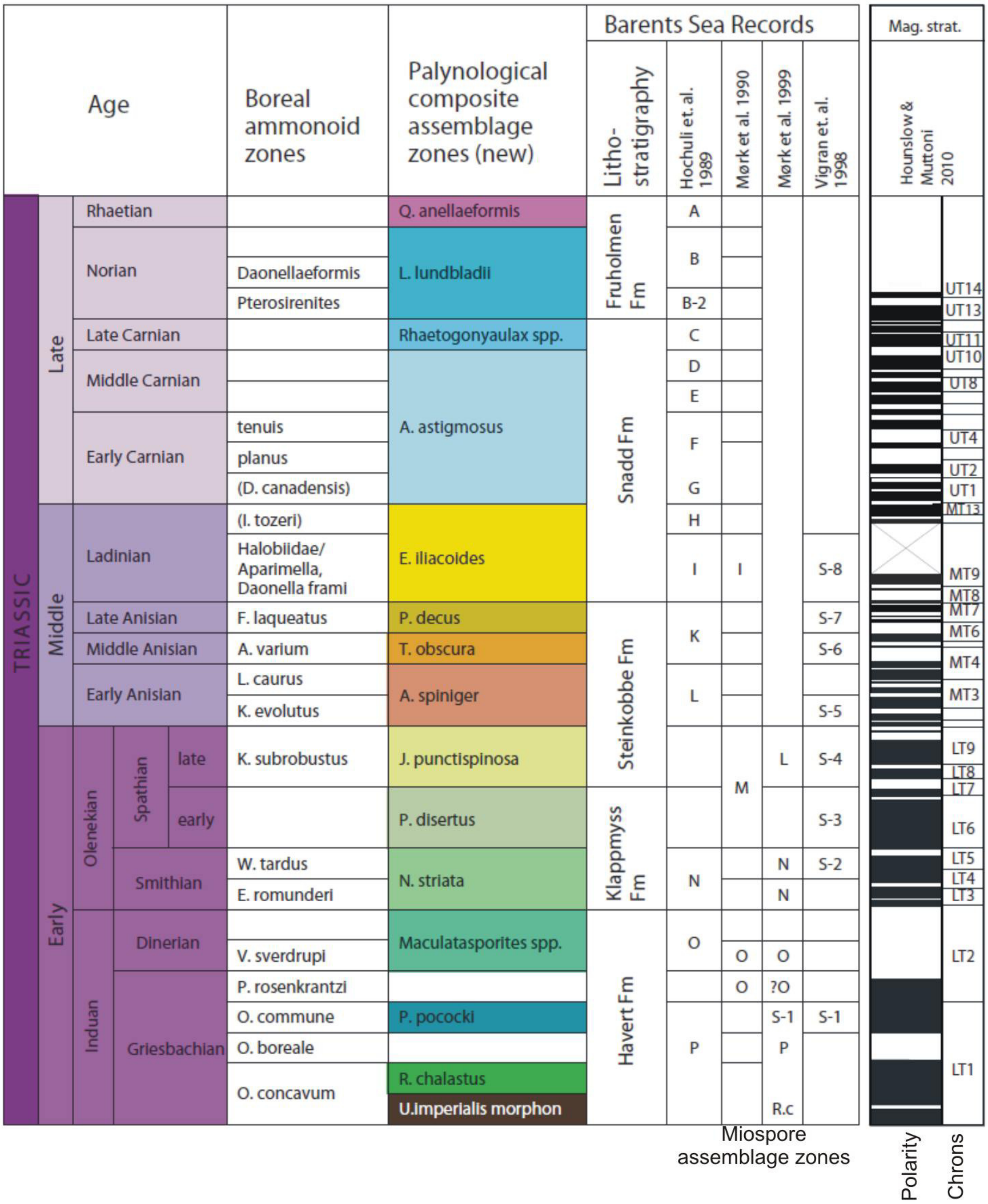

Fig. 1. Biostratigraphy and lithostratigraphy of the Barents Sea. The magnetostratigraphy is an optimistic correlation from land-based sections on Svalbard onto the biostratigraphy (From Vigran et al., Inpress). Black=normal polarity, white=reverse polarity

A detailed palynological zonation exists for this interval (Vigran *et al.* in press; Fig. 1), but lacks in part independent age control to well dated (i.e. by ammonoid or conodont or radiometric ages) sections elsewhere, hence the chronostratigraphy of the zonations are poorly understood. Other means of age control such as magnetostratigraphy (i.e. fossilised changes in the polarity of the Earth's magnetic field) are available from the Botneheia and De Geerdalen formations in central Spitsbergen (Hounslow *et al.* 2007). Magnetostratigraphy allows precise age assignments through correlating the pattern of polarity changes to sections often at lower latitudes, with more comprehensive biostratigraphy.

An ongoing study (Xu et al. inpress) has dated the Botneheia to Tschermakfjellet formation boundary (often regarded as the Ladinian – Carnian transition in Boreal stratigraphy) as 236.5±3.5 Ma based on Re-Os isotopes. These studies are made on two of the same cores as analysed in the present study. Due to the organic richness and presence of phosphate nodules we assign core 7831/2-U-2 to the Botneheia Formation, which based on palynology and ammonoids are dated to the Ladinian (Xu *et al.* in press).

The current lack of high resolution age control has implications for precise dating of any sequence stratigraphic or lithostratigraphic subdivision of the Upper Triassic in the Barents Sea region. This work address these issues by providing a chronostratigraphy for the late Triassic successions in the cores from offshore Kong Karls Land, using magnetostratigraphy combined with available bio- isotope- and lithostratigraphy.

1.2 Lithostratigraphy

The area studied is close to the islands of Svalbard with its well defined litho-stratigraphical units (Figure 1;Mørk *et al.* 1999). A separate lithostratigraphy was defined for the Barents Sea by Worsley et al. (1988) based on data from the south-western Barents Sea which was the best studied area at that time. In the reappraisal of the lithostratigraphy of Svalbard (Mørk et al. 1999), units at group levels were assigned throughout both Svalbard and the Barents Sea, while different terminology was retained for the offshore and onshore Svalbard areas. Due to the localisation of the drilled areas offshore Kong Karls Land, quite close to the Svalbard archipelago, and a long distance from the type areas of the SW Barents Sea we use a mixed lithostratigraphical subdivision here based on both established systems.

The cores analysed in this report represents the Botneheia, Tschermakfjellet De Geerdalen and Snadd formations. Below we summarise the characteristics of these units (Fig. 1).

The Botneheia Formation forms the upper part of the Sassendalen Group in central and eastern Spitsbergen as well as the eastern islands of Edgøya and Barentsøya (Mørk *et al.* 1999, Krajewski 2008). In these areas it is regarded as covering the Middle Triassic-Anisian and Ladinian Stages (Dagys and Weitschat 1993). The unit consists of dark very organic rich shales, often with abundant bivalves in the upper part. Phosphate nodules occur throughout. In the Barents Sea its equivalent is the Steinkobbe Formation which has a very similar occurrence, however, this organic rich sedimentation started in the early Spathian, i.e. almost one stage earlier than on Svalbard (Vigran *et al.* 1998).

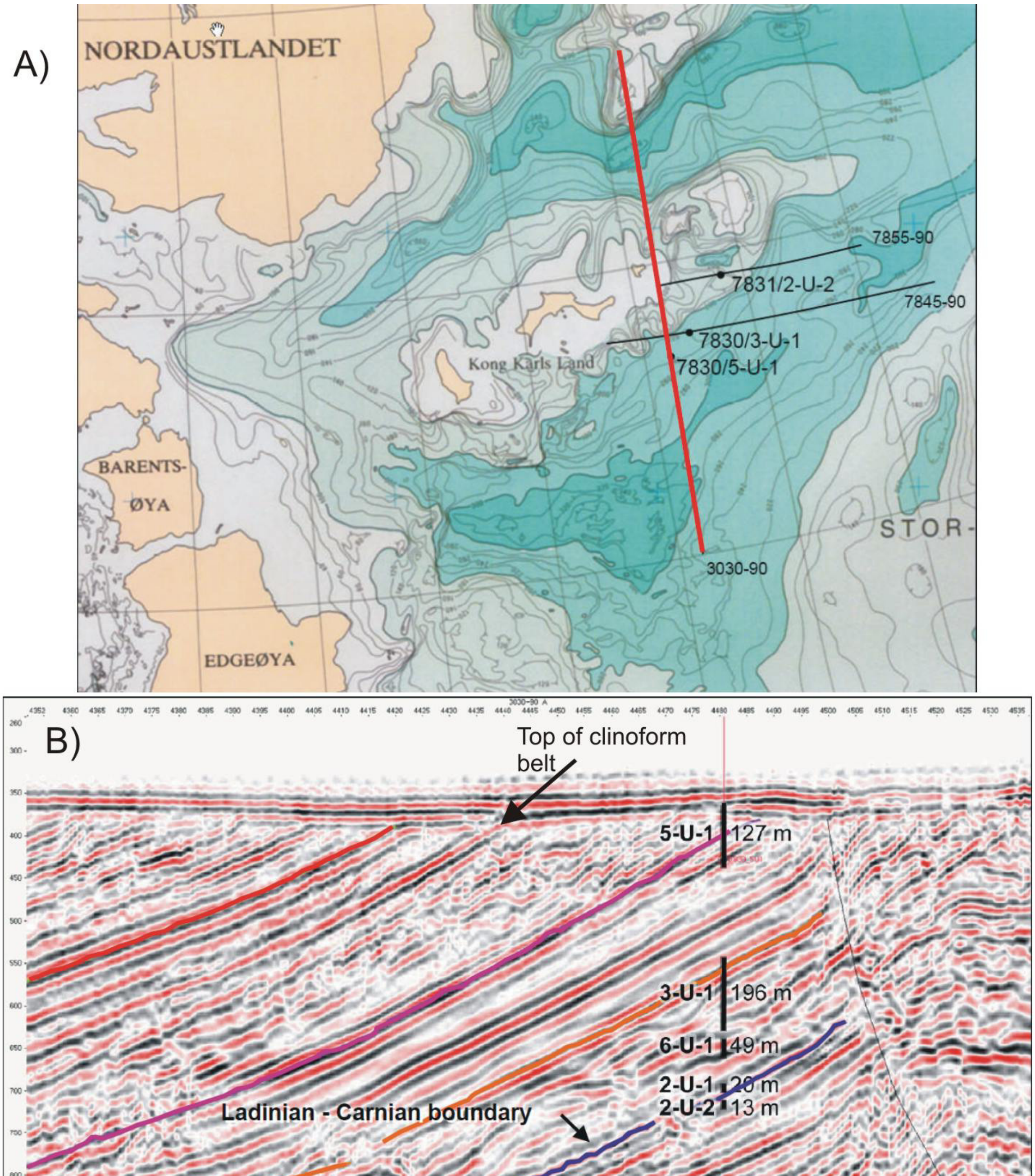

Fig. 2 a) The location of the cores south of Kong Karls Land. B) The location of the wells transferred to a seismic section, with seismic section shown in red in b) (from Riis *et al.* 2008).

The Tschermakfjellet Formation is the basal unit of the Kapp Toscana Group on Svalbard and represent a pro-delta shale and siltstone with abundant siderite beds and nodules sharply overlying the Botneheia Formation (Mørk *et al.* 1999). It is dated on Svalbard by ammonoids as early Carnian (Dagys and Weitschat 1993). The boundary between these two mudstone units is a submarine hiatus or condensed interval, and may represent a time gap in some areas, however no erosion is observed. The basal beds above the boundary have recently been dated as 236.5±3.5 Ma based on Re-Os isotopes (Xu *et al.* inpress), studies made on the same cores as analysed in this work.

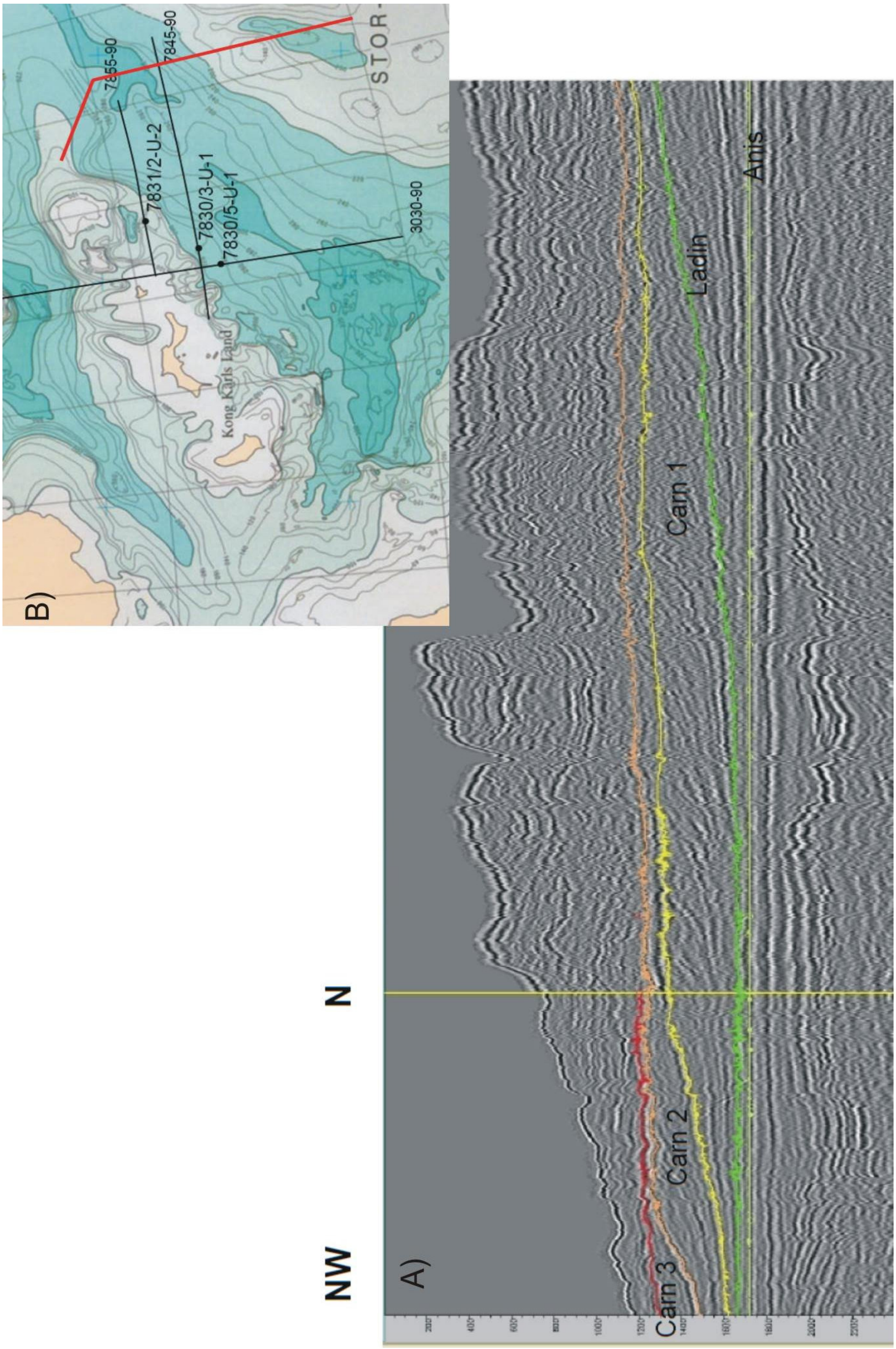

Fig. 3. A) Triassic delta lobes (flattened on top of Anisian reflector). B) Location of seismic section (marked in red). From Riis *et al.* (2008).

The Tschermakfjellet Formation grades into the De Geerdalen Formation and the boundary is taken at the top of the first prominent sandstone (Mørk *et al.* 1999). This definition makes the boundary probably diachronous as different sandstones are present at different levels at different localities dependent on delta lobe switching of the fluvial channel systems seen in the De Geerdalen Formation. The De Geerdalen Fm consists of repeated coarsening upward sandstone bodies separated by shales. The sandstone bodies vary in thickness from a few metres up to 30 m and represent development of deltaic channel sandstones, coastal and shoreface sandstones and offshore sandstones (Mørk *et al.* 1982, Riis *et al*. 2008). The major sandstone bodies in the lower unit can show great thickness variations laterally, over a distance of several hundred metres, as a result of the development of channel systems. The chronostratigraphic relationships of the western and eastern units on Svalbard are not clear, and it is not clear how these units may relate to prospective units in the Barents Sea. The overlying Triassic part of the Wilhelmøya Subgroup (Fruholmen Fm in the Barents Sea) is shale dominated and seems to be all of Norian age, based on a few ammonoids and palynostratigraphy (Vigran *et al*. in press.).

1.3 Stratigraphy of the northern Barents Sea

In the Barents Sea the Snadd Formation is equivalent to both the Tschermakfjellet and De Geerdalen formations, and it base is in the early Ladinian. The Snadd Formation consists of shales, siltstones and paralic sediments representing a gradual infill of the sedimentary basin by sediment. The Snadd Formation and its equivalents on Svalbard represent the same depositional system and grade into each other (Mørk *et al*. 1999, Riis *et al*. 2008, Glørstad-Clark 2010).

NPD has drilled cores through the Upper Triassic succession of the northern Barents Sea close to Kong Karls Land, in Hopendjupet and on Sentralbankhøgda (Table 1; Fig. 2). In this succession a series of clinoform belts are prograding north-westwards on the northern Barents shelf (Riis *et al.* 2008, Glørstad-Clark 2010, Høy & Lundschien, 2011). These are especially well developed in the Carnian-Norian succession (Fig. 3), and form a potential framework for sequence stratigraphical subdivision (Riis *et al.* 2008, Glørstad-Clark *et al.* 2010). The close relationship between the De Geerdalen Formation as exposed on Hopen, the south-eastern most island of Svalbard and the Snadd Formation of the Barents Sea is demonstrated by Klausen and Mørk (submitted) who demonstrate how the river channels exposed on Hopen are similar to seismically interpreted channels of the Snadd Formation close to the Norwegian Mainland. Magnetostratigraphy may assist in the correlation of the different sequences between the drilled areas, as the cores (based on seismic and facies interpretation) seem to overlap in age interval. Paleontological methods cannot resolve such detailed correlations.

2. Magnetostratigraphy of the Middle and Upper Triassic

The geomagnetic polarity timescale for the Middle and Upper Triassic comprises some 40 major normal-reverse polarity couplets (MT1 to MT13, UT1 to UT 28; Fig. 4), with a magnetic polarity boundary (i.e. between reverse (white) and normal (black) polarity) on average every ~0.26-0.53 Ma (Hounslow & Muttoni, 2010). The biostratigraphy, to which it is related, is based mainly on conodonts from numerous Tethyan sections with support from successions such as the Newark Supergroup from eastern USA (Hounslow & Muttoni, 2010). Distinctive polarity changes in the time-scale of the late Triassic are the long reverse polarity-dominated interval during the early Norian (magnetochrons UT13r to UT16r), and the normal polarity dominated mid and upper Rhaetian. The Carnian has magnetozones of roughly equal duration, with more dominant normal polarity in the latest Carnian and latest Ladinian (Fig. 5).

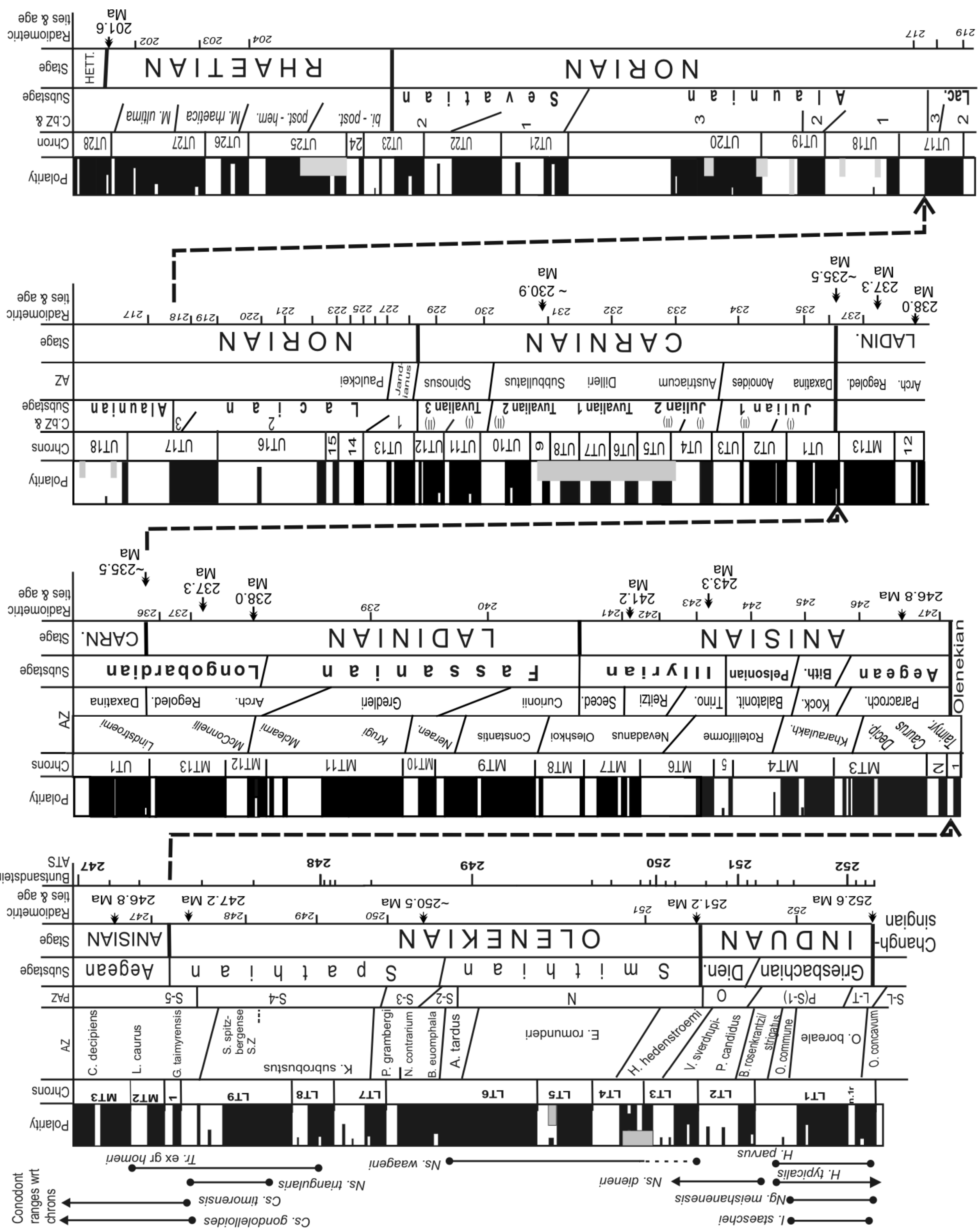

Fig. 4 The magnetic polarity timescale for the Triassic from Hounslow & Muttoni (2010). The magnetozone normal-reverse polarity couplets are labeled as LT, MT and UT for the Lower, Middle and Upper Triassic. ATS=astronomical time-scale. Radiometric U/Pb dates shown as black arrows, interpolated ages as ticks. Normal polarity=black, reverse polarity=white bars. Grey bar are level of uncertainty.

The predominantly biostratigraphic definition of the Ladinian-Carnian (Mietto *et al.* 2012) and Carnian-Norian boundaries (as used by Hounslow & Muttoni, 2010), does not simply correlate onto the boreal, ammonoid based stage definitions often used in the Barents Sea. For example, the Ladinian-Carnian boundary defined by the international community (at the FA of the ammonoid *Daxatina canadensis* at the Stores section in Italy; Mietto *et al.* 2012) may correlate on Svalbard to a level below the Tschermakfjellet Fm, within the uppermost parts of the Botneheia Fm.

The existing magnetostratigraphy from the upper Triassic in the Vendomdalen area of central Spitsbergen (Hounslow *et al.* 2007; Fig. 5) has provided crucial insight into the chronostratigraphy of the Tschermakfjellet and De Geerdalen formations in this area (Fig. 5). This has indicated the rapid sedimentation rate of the lower parts of the De Geerdalen Fm corresponding to magnetochron UT2n in the Triassic timescale (Fig. 5). The base of the Isfjorden Member appears to corresponds to an interval in the mid Carnian, with the Isfjorden Mbr displaying a lower sedimentation rate, evident by much thinner normal magnetozones, and appears to be upper Carnian, although the confidence in this age assigment is low. The magnetic polarity stratigraphy through the upper parts of the De Geerdalen Fm and Wilhelmøya Subgroup on Spitsbergen is so far unknown.

3 Well and Sample Information

Core Name	**7830/3-u-1**	**7831/2-u-1**	**7831/2-u-2**
Sampling depth range	199.55m – 4.21m	27.70m – 9.12m	18.64m – 6.62m
Number of specimens measured	118	21	26
Number of sampled horizons	103	22	20

Table 1. Summary of relevant core and sampling information (see Fig. 2 for core location details).

Area/core	**Formation**	**Core length (m)**	**Probable age interval**
Offshore Kong Karls Land, collected, 2005			
7831/2-U-2	Botneheia	14	late Ladinian
7831/2-U-1	Tschermakfjellet - De Geerdalen	20	late Ladinian - earliest Carnian
7830/3-U-1	Snadd	197	early Carnian

Table 2. Summary of NPD northern Barents Sea core examined in this study.

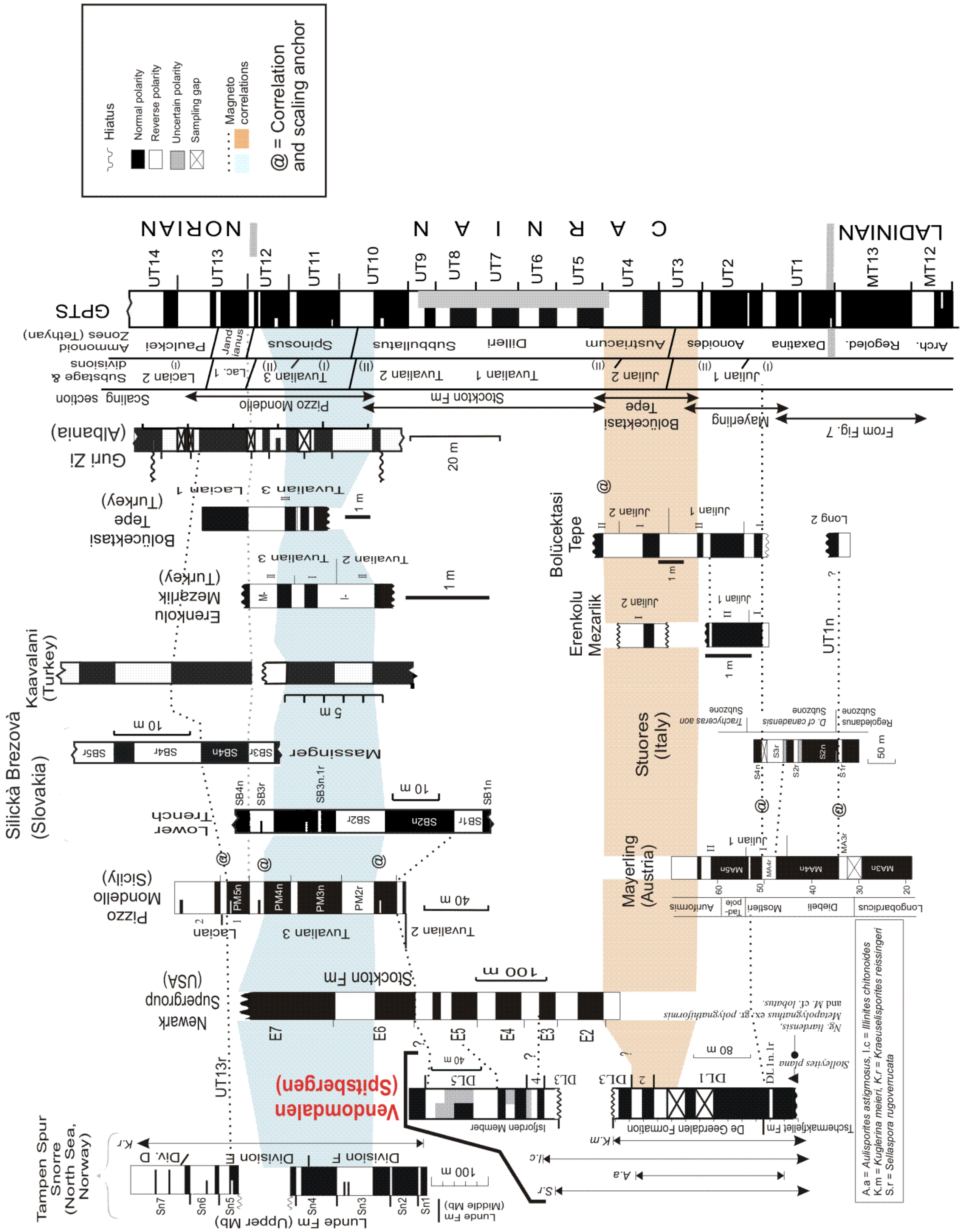

Fig. 5. Global bio-magnetostratigraphic data for the Carnian, also showing the magnetostratigraphic data for the Dalsnuten section in Vendomdalem (central Spitsbergen), the only published data from the Carnian of Svalbard. From Hounslow and Muttoni (2010). Ranges of selected palynomorphs shown on Norwegian data.

3.1 Magnetostratigraphic Sampling

Sampling horizons for magnetostratigraphy were selected based on the following principles:

a) To obtain an approximate equal time-spacing of samples throughout the cored interval.

b) All core fragments were reassembled, where possible, into a continuous 'core run' with a common azimuthal orientation. This reassembly was performed in order to be both confident that core fragments were not inverted, and so that in some core sections samples were collected so that they possessed a common azimuthal orientation. This aids interpretation of the magnetostratigraphic data.

c) Apparent bedding dips were taken on the front and side of the core, in order to measure the apparent dip direction. The bedding dip values were generally applied to the palaeomagnetic measurements to modify the palaeomagnetic directions into coordinates with respect to palaeohorizontal. The assumption being that the apparent, relative dip directions measured on the core represent the consistent bedding dips seen in seismic section. These could be reconstructed, if we could orient the sampled-core segments using the palaeomagnetic method. In some cases, the dips were interpreted as depositional dips (i.e. cross-bedding), and therefore not used in correcting the palaeomagnetic directions.

Samples were taken from the core by cutting sections out of the core, cut dry on a diamond saw. All samples were marked with a reference fiducial, directed up-core. Any fragmented samples were glued together using Na-silicate or PVA glue once at Lancaster University.

Palaeomagnetic specimens were prepared by trimming the samples using a water-lubricated circular saw. In most cases the centre of the sample was used for analysis, however, in some cases a sister specimen was also cut from the remainder of the material, if measurements on the primary specimen were inconclusive. A variety of lithologies were sampled including sandstones, claystones and siltstones.

4 Palaeomagnetic procedures

Demagnetisation procedures were designed to achieve two objectives:

1. Extraction of the thermoviscous remanent magnetisation (TVRM) from the specimens. If this was acquired during the Brunhes chron (i.e. since 0.78 Ma), then the direction of this would allow reorientation of the core segments back into their *in situ* position, assuming the TVRM declination was directed north. The expected inclination (Inc.) for the Brunhes-age magnetic field at the latitude of the core sites is 84.3^{o} (core 7830/03-u-01) and 84.4^{o} (cores 7831/02-u-01, 7831/02-u-02).
2. Extraction of the Triassic magnetisation direction- this is referred to as the characteristic remanence magnetisation, or ChRM. The expected directions of the ChRM in these cores are shown in Table 3, assuming no vertical axis tectonic rotations had taken place since the Triassic.

Table 3. The expected mean Triassic magnetisation from cores, based on apparent polar wander path for Baltica from Torsvik & Cocks (2000). Virtual geomagnetic poles (VGP) used: 230Ma pole is longitude/latitude of 137.9/+55.8, 240 Ma pole is 147.1/+56.0.The declination (Dec.) data was used to define the expected palaeomagnetic orientation for each core.

Core	Dec (°)	Inc (°)	VGP Pole Age (Ma)
7830/3-u-1	059	68	230
7831/2-u-2	052	67	240
7831/2-u-1	052	67	240

The TVRM was typically isolated with thermal demagnetisation between 100°C, until the early stages of AF demagnetisation. For most lithologies the upper heating limit was dictated by the onset of mineralogical alteration (i.e. start of the 'susceptibility crisis'), which for many specimens began at about 200-250°C. This often prevented useful thermal demagnetisation beyond ~250°C. Magnetic susceptibility measurements were made after each heating step to characterise the susceptibility crisis. Following initial trials, identifying the crisis point, specimens were subsequently AF demagnetised, starting just prior to the on-set of the susceptibility crisis in 5 -10 mT steps up until magnetic fields of about 80 to 100 mT.

4.1 Analysis of the demagnetisation data

Both the TVRM and ChRM directions were extracted from the demagnetisation data using principle component analysis as implemented in the LINEFIND software (Kent *et al.* 1983). This program allows a quantitative assessment of the ChRM and TVRM directions, utilising the uncertainty in the multiple measurements of each magnetisation. It also allows a user to assess the demagnetisation data in terms of a likely magnetisation error model which best describes the data. As a result of the ability of LINEFIND to use the magnetisation measurement variance (i.e. the uncertainty), it is able to deal effectively with specimen data, which appear to have scattered points on the Zijderveld plots (see Appendix).

4.2 Extraction of TVRM directions

Thermoviscous overprints could not be extracted from all specimens, overall core 7830/03-u-01, contained the most clearly defined TVRM directions (Table 4). The TVRM is seen as a steep down-wards directed magnetisation which dominates the NRM directions of most specimens. Mostly the TVRM was removed during thermal demagnetisation steps starting from 100°C, with some starting as high as 210°C. The demagnetisation range for the TVRM was mostly between 100 °C up until the initial or mid stages of AF demagnetisation steps.

After initial analysis on core 7830/3-u-1 it was clear that the TVRM could not be used to orient the cores, as originally had been planned. Using the TVRM produced scattered bedding dip directions, indicating that the TVRM declination was not a reliable indicator of north (this assumes the bedding dips are consistent in each core). Orienting the core using the TVRM probably does not work for these cores because the very steep TVRM directions are variably contaminated with other magnetisation components (i.e. of Triassic age or drilling induced?). This interpretation of the TVRM declinations is similar to that in the overprint magnetisation directions seen on Spitsbergen, where contamination with a dual polarity Mesozoic or Cenozoic magnetisation is inferred for the overprint (Hounslow & Nawrocki 2008).

On the basis of the apparently down-directed nature of the TVRM, three core segments were thought to be inverted. These are at 16.63m in 7831/2-u-2, and 121.80m, 94.82m in 7830/3-u-1. The resulting palaeomagnetic directions were corrected for this.

Table 4. Statistics about demagnetisation behaviour of specimens. S1.. S3 and T1.. T3 are types of demagnetisation behaviour (See section 4.3). TVRM= Thermo-viscous remanent magnetisation.

Core	**Demagnetisation class**			
	% with S1,S2,S3	**%with T1,T2,T3**	**% with TVRM**	**Number of specimens**
7830/3-u-1	9,26,23	0,13,27	63	119
7831/2-u-2	42,23,8	4,11,11	35	26
7831/2-u-1	38,24,19	5,14,0	18	21

4.3 Extraction of the ChRM (Triassic magnetisation)

Specimen behaviour during demagnetisation was classified into the following three types:

a) S-Type: A ChRM could be defined, using three or more points on a straight line segment on a Zijderveld diagram, commonly directed through the origin. The ChRM was commonly defined, starting with the last thermal demagnetisation steps (240-300^{o}C), or the early stages of AF demagnetisation (*Figs. 6,7*). The end range typically went to the 60-75 mT steps. In some specimens noise imparted by the AF demagnetiser at high fields (>~75mT), often precluded origin-fitting to the origin. Specimens were visually classified into three S-type groups (S1, S2 and S3), with S1 having the least noisy line fits and S3 the most noisy. S-type behaviour is seen in >55% of specimens (*Table 4*).

b) T-Type: Specimens exhibited a great-circle path towards an interpreted Triassic-like inclination. Sometimes a Triassic-like direction could be inferred, based on the direction of the TVRM, (i.e. ChRM ~50-60^o anticlockwise of the TVRM declination), or if not available, from the expected Triassic inclination (Table 3; Fig. 7). Specimens with T-type behaviour were classified qualitatively into best quality (T1) and inferior quality (T2, T3) great-circle trends, based on the directional scatter. Some 20-40% of specimens displayed this behaviour, dominated by specimens inferred to have reverse polarity Triassic magnetisations. For these specimens great circle planes were determined through the demagnetisation data using LINEFIND. Such demagnetisation behaviour is very common in Triassic outcrop sections on Spitsbergen (Hounslow et al. 2007, 2008b).

c) X-Type: Specimens exhibited either i) erratic directional behaviour, or ii) the persistence of the TVRM magnetisation to the highest demagnetisation stages. This type is identified in only two specimens measured from 7830/3-u-1, and derived no useful orientation or magnetic polarity data.

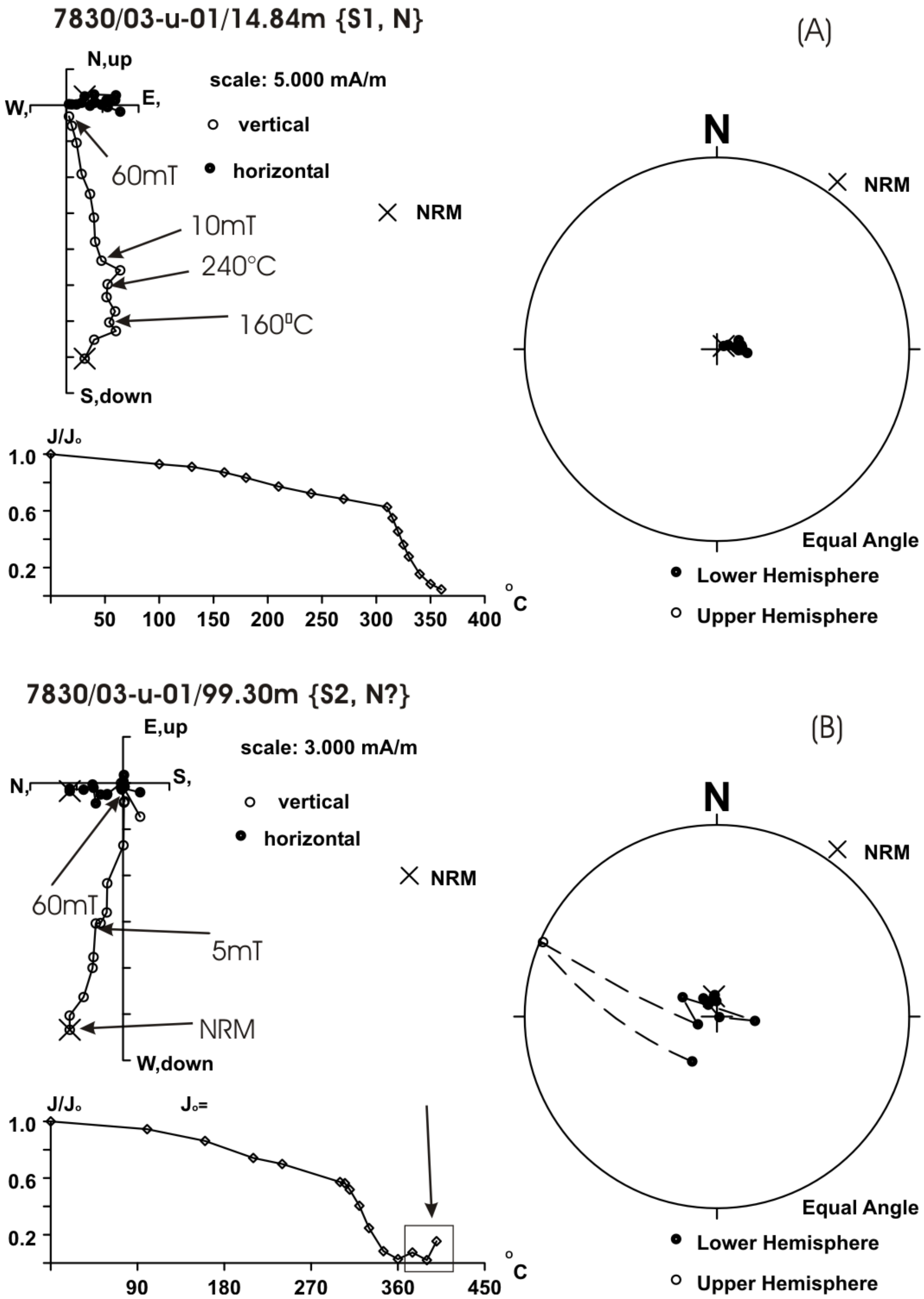

Figure 6. Examples of class S1 and S2 behaviour. A) The TVRM is best defined between 160°C and 240°C, followed by a ChRM interpreted to be a Triassic normal from 10 mT to 60 mT with an inclination of 64° (corrected for bedding dip). The polarity is unambiguously normal, hence assigned N polarity quality. B) A possible TVRM is evident from the NRM to 5 mT through the thermal demagnetisation phases. The ChRM (Triassic N?), which has an inclination of 72°, can be isolated between 5 mT – 60 mT and is to the relative-west of the apparent TVRM. 'N' on the plots is the fiducial direction on the core segment.

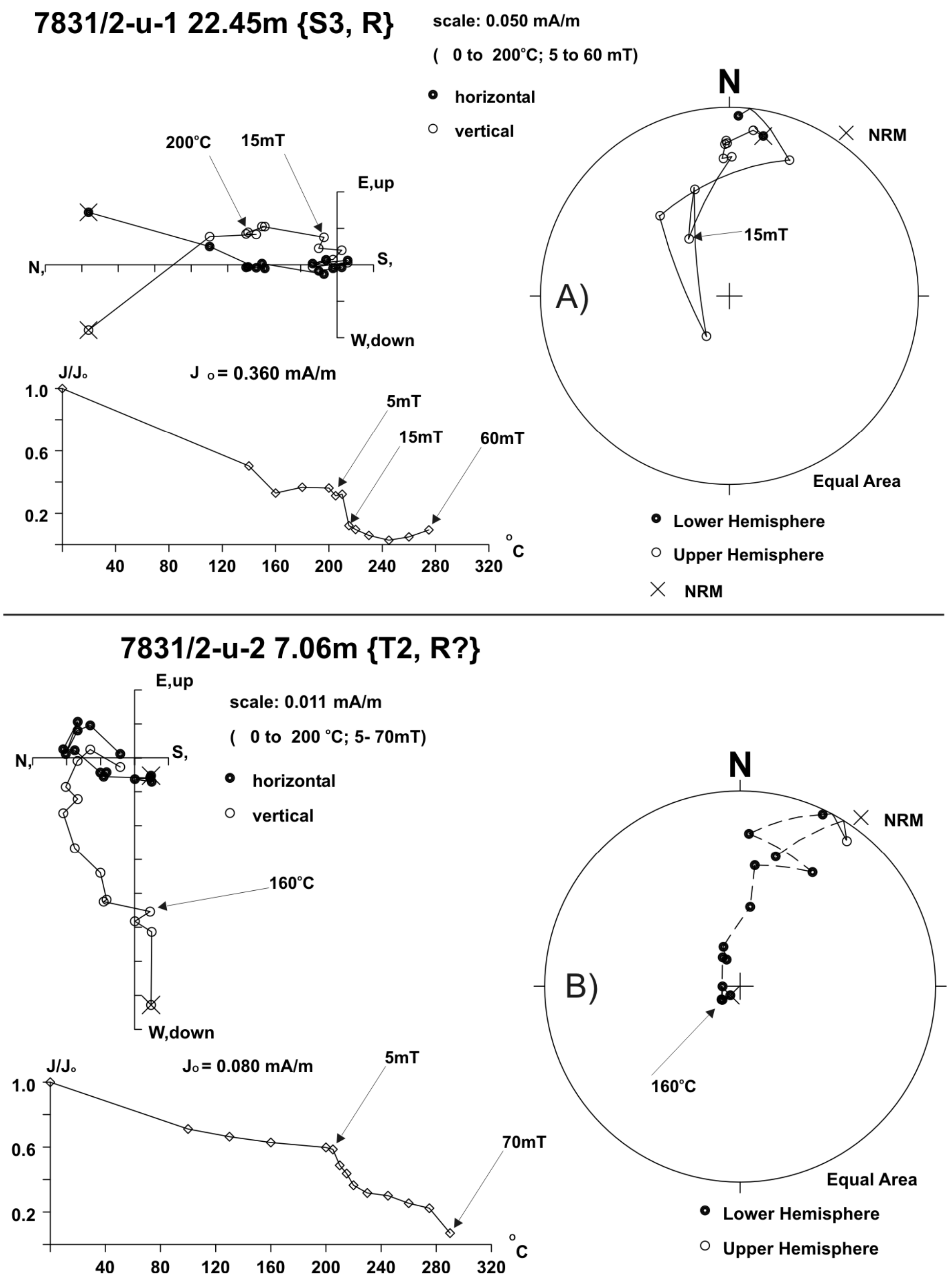

Figure 7. Examples of class S3 and T2 behaviour. A) No evidence of a TVRM is present, only a reverse polarity magnetisation from 15mT to the origin, with an inclination of -57^{o} (polarity R), which is interpreted as a Triassic reverse.. (B) Specimen shows a relatively 'southerly'-directed TVRM from the NRM to 160^{o}C (core coordinates of $224,+88^{o}$). This is followed by a great circle trend towards the relative NNE (curving trajectory on Zijderveld plot), with a probable reverse polarity which is not well defined as a stable end point. The fact that's it opposite to the TVRM direction adds weight to the reverse polarity interpretation of this specimen. Both specimens with bedding correction.

4.4 Orientation of the Palaeomagnetic Remanance

The samples were oriented with respect to geographic north using two methods:

#1. For the bulk of S-class specimens the ChRM declination was used to determine the rotation angle of the core segments, to convert directions into geographic north coordinates. This assumed that the normal polarity ChRM was oriented towards the expected VGP declination in Table 3 (reverse polarity directions are 180^{o} from these). With this rotation, we are able to orient the bedding dip directions in each core segment into geographic coordinates (i.e. with respect to 'true' north). For some specimens within a core run, or adjacent specimens with very similar apparent bedding dip directions, we pooled the mean ChRM directions from adjacent specimens to determine the mean rotation angle for that core segment (the percentage of samples we did this for is indicated in the column 'using run data' in Table 5). Since there is directional uncertainty associated with both the apparent bedding dip measurements (i.e. measured from the core) and the ChRM directions, we divided the declination dispersion equally between these two to produce a more realistic directional scatter, which reduces the scatter in the bedding dip directions, but, increases it in the ChRM declinations (Fig. 8).

#2. Using the mean of the bedding dip directions derived from method #1 we could orient most of the remainder of the specimens, by rotating the apparent bedding dip directions (measured on each core segment), into the mean bedding dip direction for that core (Fig. 8). This oriented most of the remainder of the specimens.

*Table 5. Core orientation statistics, showing the percentage of specimens oriented using either method #1 or #2 above from each core. * number inside {} indicates the number of specimens with interpreted depositional dips, which were not used in determination of the mean bedding dip direction. The percentage in column 'using 'run' data' is the percentage of all specimens from that core.*

Core	#1:%oriented using N [or R] ChRM	%oriented using 'run' data	#2:% oriented using bedding dip direction	Number of specimens*	Mean bedding dip direction (and dip)
7830/3-u-1	51 [2.5]	31	30.5	119 {6}	025 (10.7)
7831/2-u-2	58 [15]	54	27	26 {0}	034 (13.8)
7831/2-u-1	43 [33]	10	24	21 {2}	030 (33.9)

4.5. Mean directions of the geomagnetic field in the cores.

In spite of the re-orientation of the core segments using the method in Section 4.4, the ChRM directions are still dependent on the assumed VGP declination in Table 3. Hence, we cannot usefully determine an independent assessment of the geomagnetic field direction. However, we can determine the apparent mean direction from each core (Table 6). The some 10 to 14^{o} difference in the combined mean for core 7830/3-u-1 compared to 7831/2-u-2 and 7831/2-u-1 is largely a reflection of the 7^{o} difference between the expected VGP directions used in orienting the core (see Table 3).

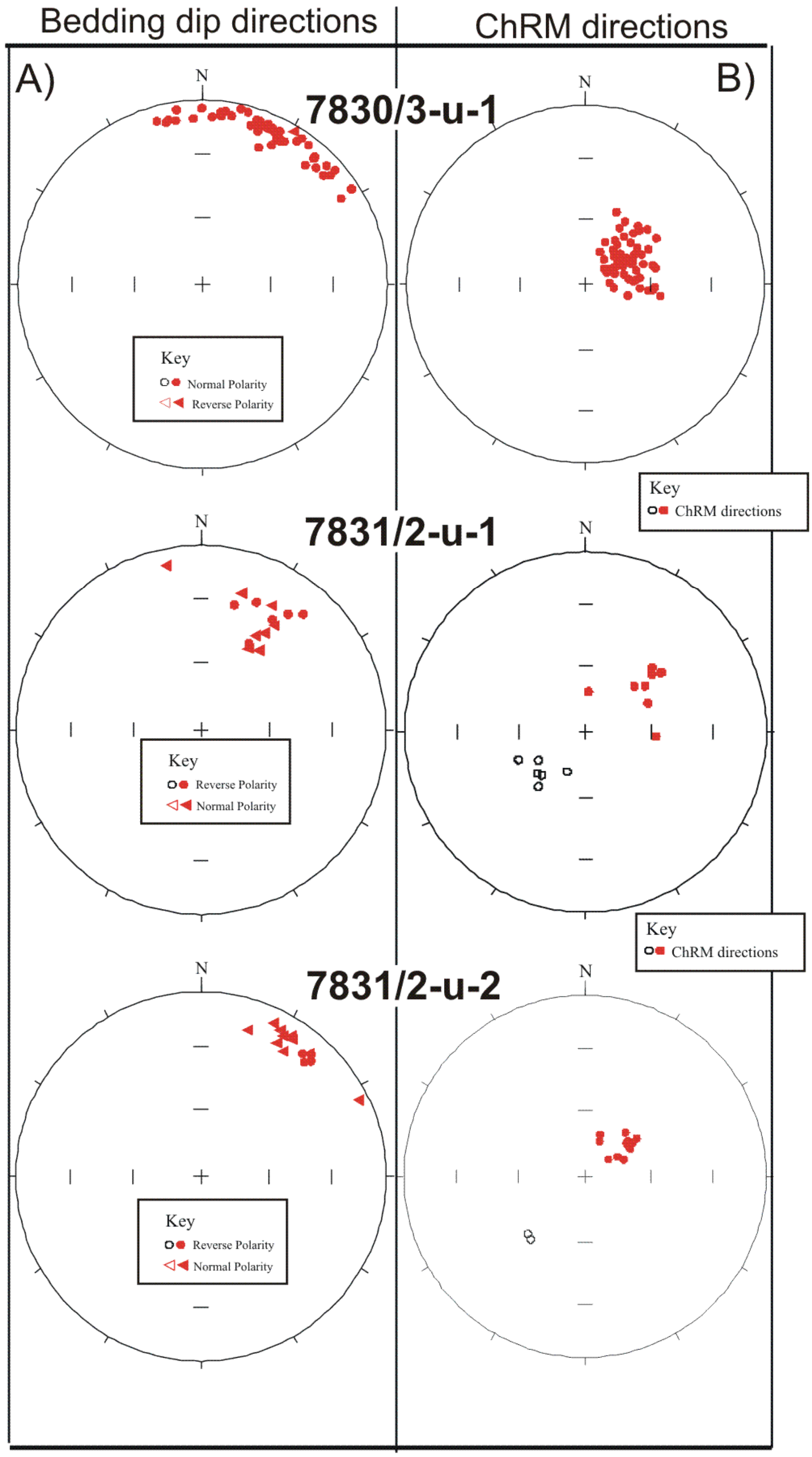

Fig. 8. A) bedding dip directions oriented using the S-class ChRM directions. B) S-class characteristic remanence directions oriented into the expected geomagnetic field direction (from Table 4). For each specimen in these plots the dispersion about the mean has been divided equally between the bedding dip direction and the ChRM direction. Filled symbols are lower hemisphere projection, unfilled symbols are upper hemisphere projection. Equal area stereographic projection.

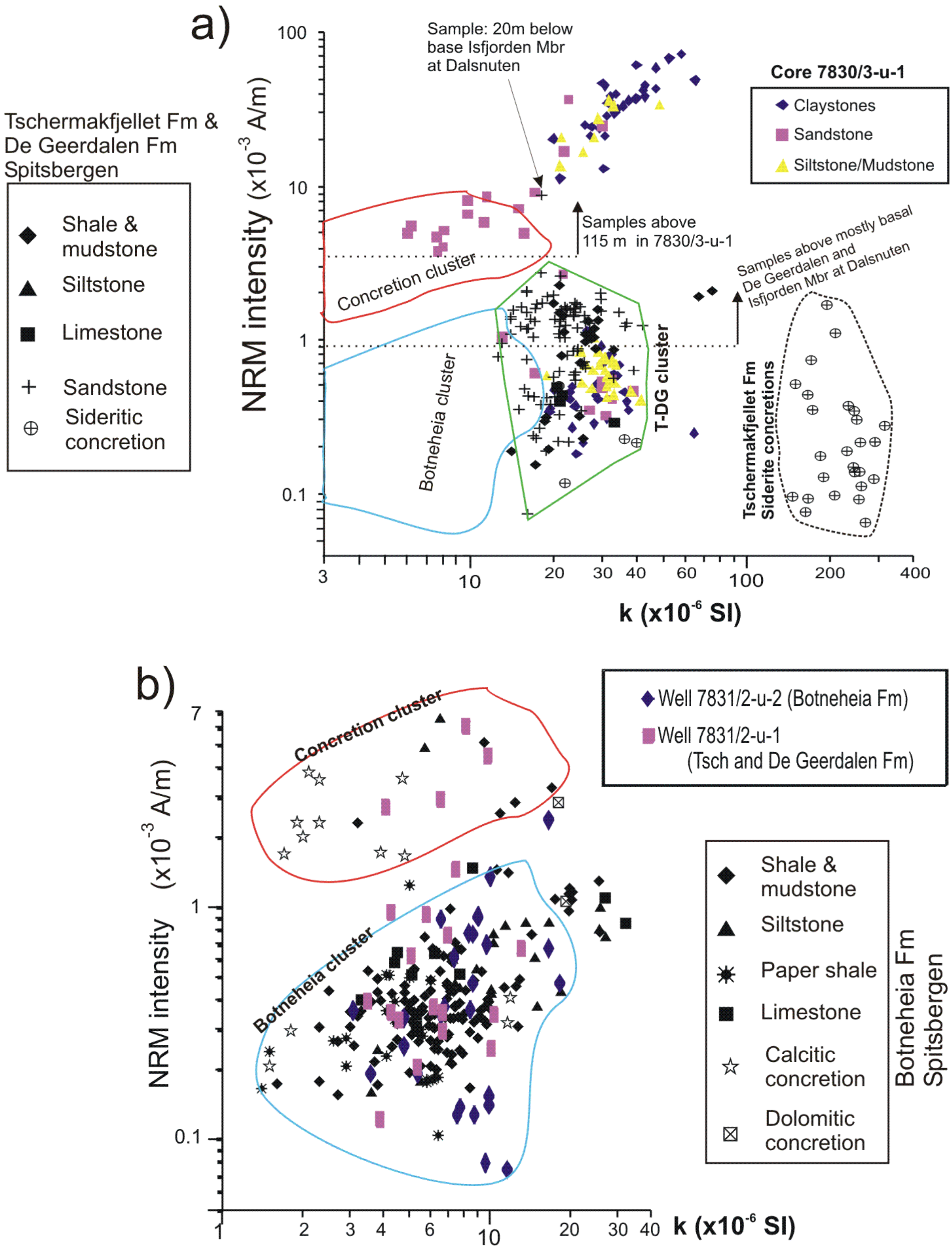

Figure 9. Magnetic susceptibility (K) versus NRM intensity for specimens from NPD and land based sections on Spitsbergen. A) For core 7830/3-u-1, and land-sections of the Tschermakfjellet and De Geerdalen formations. Concretion and Botheheia clusters from B). There is some evidence for stratigraphic seperation of NRM intensity values, which may relate to provenence differences between the low, mid and upper parts of the De Geerdalen Fm. B) For cores 7831/2-u-1, 7831/2-u-2, and Spitsbergen sections of the Botneheia Fm. Land based data from Hounslow & Nawrocki (2008).

Table 6. Mean directions of the Triassic magnetisations recorded in the cores (declination/inclination in columns 2,3 & 4). Core segment rotation using methods in Section 4.4. These are combined means using ChRM and great circle plane information (see Hounslow et al. 2007, 2008b for details). + Fisher mean using ChRM directions only (since no great circle data in this group of specimens). K=Fisher precision parameter, and α_{95} is the cone of 95% confidence about the mean direction. Nl, Np are the number of ChRM directions (Nl) and great circle planes (Np) used in defining the combined mean.

Core	Normal polarity	Reverse Polarity	R and N Combined	k (α95)	Nl/Np
7830/3-u-1	061/67	263/-60	063/67	21 (2.3)	62/35
7831/2-u-2	051/68^{+}	236/-60	053/66	60 (2.4)	17/7
7831/2-u-1	053/56^{+}	225/-61	049/59	26 (4.8)	17/3

4.6 Specimen and horizon polarity classification

Constructing a magnetic polarity record for the cores is a two stage process. Firstly the specimen data is interpreted into a likely polarity for that specimen. Secondly the polarity is assigned to each individual sampling horizon, which may comprise 1 or more specimen 'records'.

Two methods are available to assess the magnetic field polarity recorded by specimens.

1) Based on the specimen demagnetisation data, each specimen is assigned a qualitative polarity quality. This polarity quality is classed into 5 groups, 2 for each of normal and reverse polarity, with the samples labelled N (or R) showing the best quality data, and N? (or R?) poorer quality data (*Figs. 7,8*). The '?' class is for samples in which it is not unambiguously possible to interpret the geomagnetic field polarity of the specimen.
2) For those specimens which can be rotated into geographic coordinates (i.e. most specimens), using the methods in Section 4.4 an additional measure of polarity can be determined, using the virtual geomagnetic pole (VGP) latitude (Opdyke and Channell, 1996). Specimen data with a ChRM direction close to the expected virtual geomagnetic North pole for the core (i.e. normal polarity) has a VGP latitude of +90, and -90 if the ChRM direction is close to the geomagnetic south pole (i.e. reverse polarity). For the T-class specimens, the VGP latitudes were determined by using the point on the specimen great circle plane nearest the appropriate normal or reverse mean direction (i.e. those from Table 7; Hounslow *et al.* 2007; 2008a)

In order to produce a magnetozone succession through the cores, the following graphical confidence criteria were attached to the magnetozone polarity at each **sampling horizon** (i.e. polarity in Figs 10 to 13).

- Full width black or white bars correspond to normal or reverse magnetozones respectively, with which there is a high degree of confidence. This indicates at the specimen level two or more specimens **from adjacent** horizons with the same polarity and with VGP latitude > ± 30^{o}.
- Three-quarters width magnetozone indicate horizon polarity confined to two specimens with a R? or N? polarity class and T3 demagnetisation behaviour, but with VGP latitude > ± 30^{o}.
- Half-width magnetozones indicate horizon polarity confined to a single specimen and single horizon. At the specimen level, this corresponds to one specimen with good to poor polarity quality, with VGP latitude > ± 30^{o}.
- Half-width grey polarity horizons indicate two or more adjacent horizons of half-width

polarity quality, or a single sample horizon with VGP latitude < ± 30°.

In each case the boundary between magnetozones of opposite polarity are drawn mid way between the sampling horizons.

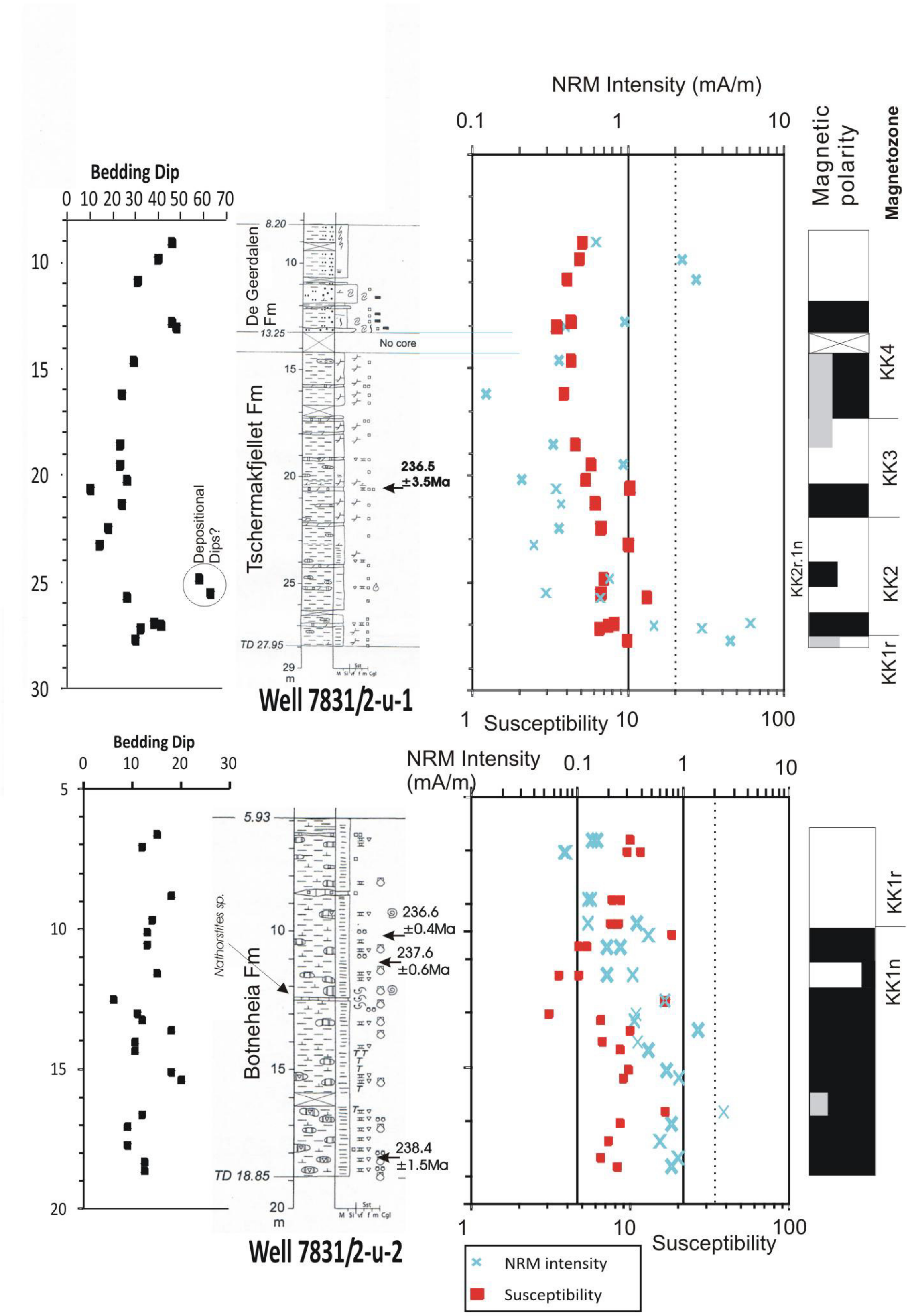

Figure 10. Summary data for wells 7831/2-u-1 and 7831/2-u-2. Including from left to right, bedding dips, lithostratigraphy, natural remanent magnetisation (NRM) intensity, magnetic susceptibility, and magnetic polarity. Polarity based on data in Fig. 12. Re/Os dates shown on the sediment log from Xu *et al.* (in press).

5 Synthesis of Results

5.1 General Magnetic Properties of the NPD cores

Magnetic susceptibility (K) and NRM intensity are strongly related to lithology and sediment body colour, with generally mudstones and claystones possessing the largest values of these parameters and sandstones generally the smallest (if the samples are close by in the cores; Figs. 9,10,11). Broadly these magnetic data when combined with data from central Spitsbergen from the Botneheia, De Geerdalen and Tschermakfjellet formations define four groups of samples:

a) A cluster with low NRM intensities (<3 $x10^{-3}$ A/m) and moderate K (12 to 50 $x10^{-6}$ SI), which predominantly includes mudstone and sandstone samples from the De Geerdalen Fm, with some samples from the Botneheia Fm (the *T-DG cluster*; Fig. 9a);

b) A cluster with low K (<12 $x10^{-6}$ SI), and low NRM intensity (<2 $x10^{-3}$ A/m), marked as the *Botneheia cluster* in Fig. 9a and 9b. This cluster predominantly represents samples from the Botneheia Fm mudstones, siltstones and shales.

c) A group of siderite-bearing samples, with NRM intensity <3 $x10^{-3}$ A/m but K >50 $x10^{-6}$ SI*),* dominantly from the Tschermakfjellet Fm on Spitsbergen.

d) A group of samples with large NRM intensities (i.e. >3 $x10^{-3}$ A/m), which includes samples from the upper-part of core 7830/3-u-1, samples from 7831/2-u-1 and calcite concretions ('*concretions cluster*') from the Botheheia Fm. This cluster shows a positive approximately linear relationship between K and NRM intensity (Fig.9a).

A *number of competing* factors related to magnetic-mineral abundance, and its mineralogy source probably account for these variations within the rocks.

1) In the grey-coloured lithologies the remanence carrying mineralogy is mostly in oxide form as magnetite, and contributes to the susceptibility but more importantly entirely to the remanence (i.e. NRM intensity). If the Fe-oxide content was entirely responsible for the magnetic susceptibility, there would normally be a positive relationship between NRM intensity and K values. The fact that only samples with NRM intensity >3 $x10^{-3}$ A/m show this kind of relationship indicates there are other minerals responsible for the magnetic susceptibility variations when NRM intensity is below 3 $x10^{-3}$ A/m (Fig. 9a).

2) Some types of Fe-bearing minerals such as chlorites, micas, siderite and ferroan dolomite can contribute to the magnetic susceptibility, but do not contribute to the NRM intensity. The few grey-coloured samples with K >50 $x10^{-10}$ m^3 , but NRM intensity < 3 $x10^{-3}$ A/m are likely to be rich in siderite, which was also observed in the NPD cores (Fig. 9a).

3) The content of iron oxide and Fe-bearing silicates is often strongly related to grain size of the lithologies, hence magnetite (and haematite?) is often more abundant in siltstones and shales compared to sandstones (Figs. 9a, 11). Hence, the larger magnetic susceptibility for the mudstones compared to the sandstones- particularly marked for specimens that have depths less than 115 m in core 7830/3-u-1 (Figs. 9a, 11).

4) The separation of samples into groups with less than and greater than NRM intensity ~2 $x10^{-3}$ A/m, is probably related to better preservation of Fe-oxides in those samples with NRM intensity >2 $x10^{-3}$ A/m. Some dissolution of Fe-oxides is normal during early diagenesis, and it is likely that those samples with NRM intensity <2 $x10^{-3}$ A/m have been more severely impacted by Fe-oxide removal. The greater

preservation of Fe-oxides for those samples with NRM intensity >2 x10^{-3} A/m is likely related to a) isolation from pore fluids within early diagenetic concretions, b) very rapid sedimentation rates allowing sediment to pass through the early stages of diagenesis much quicker than normal, so the Fe-oxides had less exposure to the destructive early phases of diagenesis. An alternative, but perhaps less likely alternative is that the NRM intensity may in part reflect provenance differences, since at Dalsnuten in central Spitsbergen those samples with NRM intensity >0.9 x10^{-3} A/m generally come from the basal and upper (Isfjorden Mbr) parts of the De Geerdalen Fm (Hounslow et al. 2007).

5.2. Chronstratigraphy of the Kong Karls Land cores

The resulting magnetozones from these cores are labelled (KK for Kong Karls Land) from the oldest sediments in core 7831/2-u-2 to the youngest sediments in core 7830/3-u-1 (Figs. 12, 13).

The data from core 7831/2-u-2 define two major magnetozones (KK1n and KK1r), with a single sub-magnetozone (KK1n.1r) from a sample at depth 11.58 m (Fig. 12). All the Re/Os dates (Xu *et al.* in press) occur within the normal magnetozone KK1n implying that this magnetozone is at least some 1.8 Ma duration, when the average magnetozone duration in the mid-Triassic is some 0.23 Ma and the Ladinian is some 5 Ma duration (Hounslow & Muttoni 2010). The ammonoid ex gr. *Nathorstites sp*. Juv., at around 12.3 m in the core suggests this part of the Botneheia Fm may be equivalent to either the late Ladinian N.E Asian ammonoid zones (*Nathorstites mclearni* and *N.mconnelli* zones) or the earliest Carnian (*Nathorstites lindstroemi*) NE Asian ammonoid zone (Dagys Konstantinov, 1995).

The data for core 7831/2-u-1 define 6 major magnetozones (KK2n to KK4r; Fig. 12). The oldest magnetozone (KK1r) is defined by only a single specimen with good quality data. More uncertain (greyed) intervals in this core correspond to lesser number of sister specimens from the same horizons. The sub-magnetozone KK2r.1n from sampling at depth 24.85 m occurs in an interval of apparently very steep bedding dips from this level to 25.50 m (Fig. 10). Because of these unusually steep dips the bedding-tilt correction was not applied in these two cases, and there is more uncertainty about the polarity at these two levels, in spite of the fact that the apparent bedding dips appear to be very similar, and the data together suggest these two levels are of opposite polarity. The Re/Os data (Xu *et al.* in press) indicate a date for magnetozone KK3n of 236.5 ±3.5 Ma (Fig. 10).

The data for core 7830/3-u-1 define 8 magnetozones (KKr5 to KK9n), and three sub-magnetozones (KK7n.1r, KK8r.1n and KK9n.1r). The major magnetozones are generally well defined in multiple sampling levels, whereas the sub-magnetozones are defined by single horizon sampling at 179.98 m, 149.28 m and 15.05-15.43 m. Sub-magnetozones KK7n and KK8r.1n are defined by only single specimens, whereas KK9n.1r is defined by single specimens at two separate horizons. The base of sandstone Unit G in this core marks the transition between KK7n and KK7r (Fig. 11), and for this reason probably represents a significant hiatus in this core. The dramatic erosional truncation observed in the core at 170.83 m may represent a second significant hiatus, but the polarity transition from KK7r to KK8n occurs a little higher in the core between 168.38 m and 169.67 m. The boundary between magnetozones KK9n.1r and KK9n.2n occurs between samples at 15.05 m and 14.84 m again a little younger in the core than the base of Unit K at 15.11 m. The *?Stolleyites* sp. in this core at around 136 m indicates this part of the core should correlate approximately to the basal Tschermakfjellet Fm in central Spitsbergen (Hounslow *et al*. 2007), and should be a little younger than the base of the Carnian (Mietto *et al.* 2012).

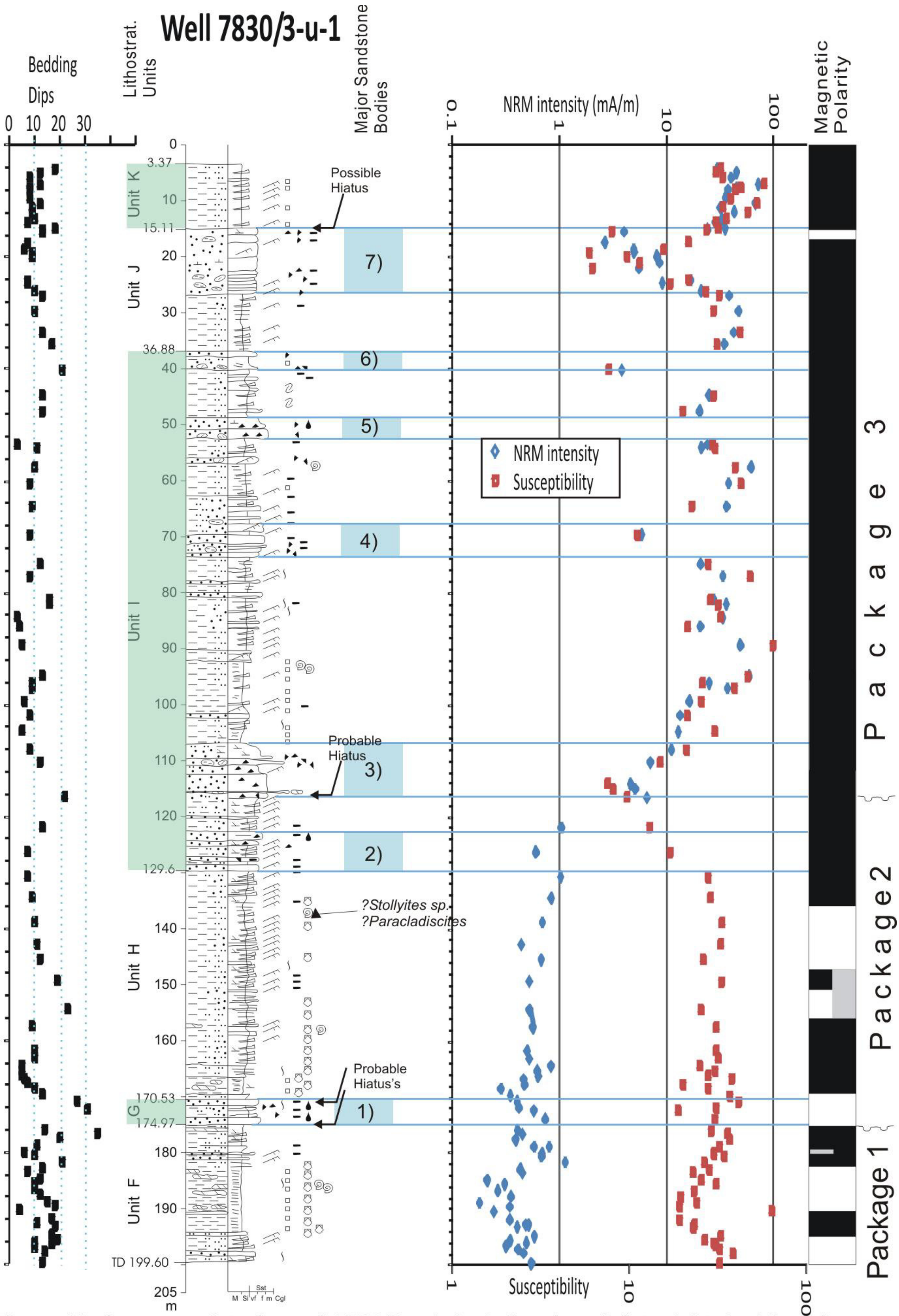

Figure 11. Summary data for well 7830/3-u-1. Including from left to right, bedding dips, lithostratigraphy, log and major sandstone bodies, natural remanent magnetisation (NRM) intensity and magnetic susceptibility, and magnetic polarity. Polarity based on data in Fig. 13.

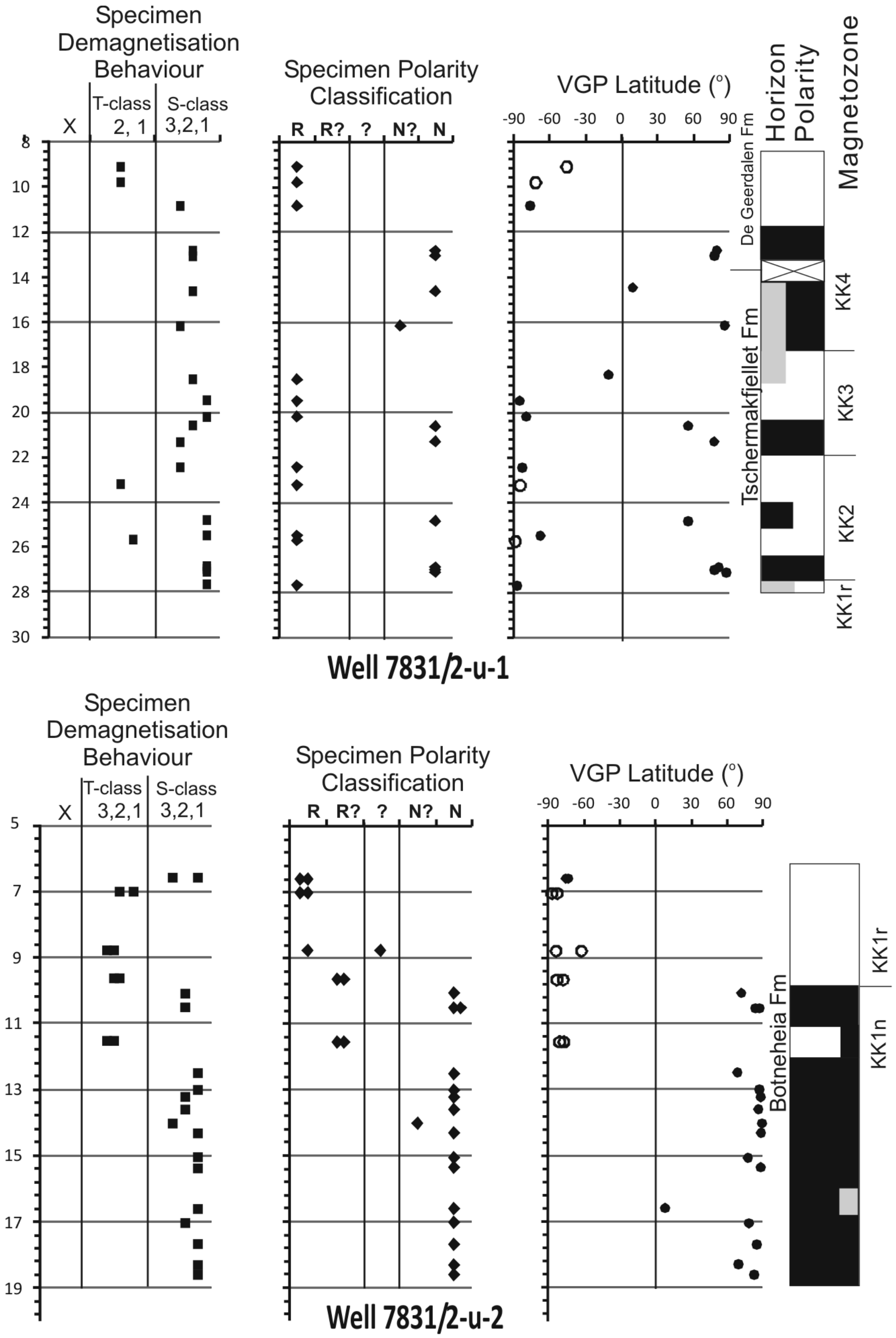

Figure 12. Summary Palaeomagnetic data from wells 7831/2-u-1 and 7831/2-u-2. Demagnetisation behaviour described in text. Specimen polarity is the interpreted polarity for all measured specimens, with R and N grades indicating high quality data, R? and N?, lower quality and ? Indicating no interpretation possible. VGP latitude is the latitude of the specimen VGP direction with respect to the mean palaeopole position, with positive values indicating normal polarity.

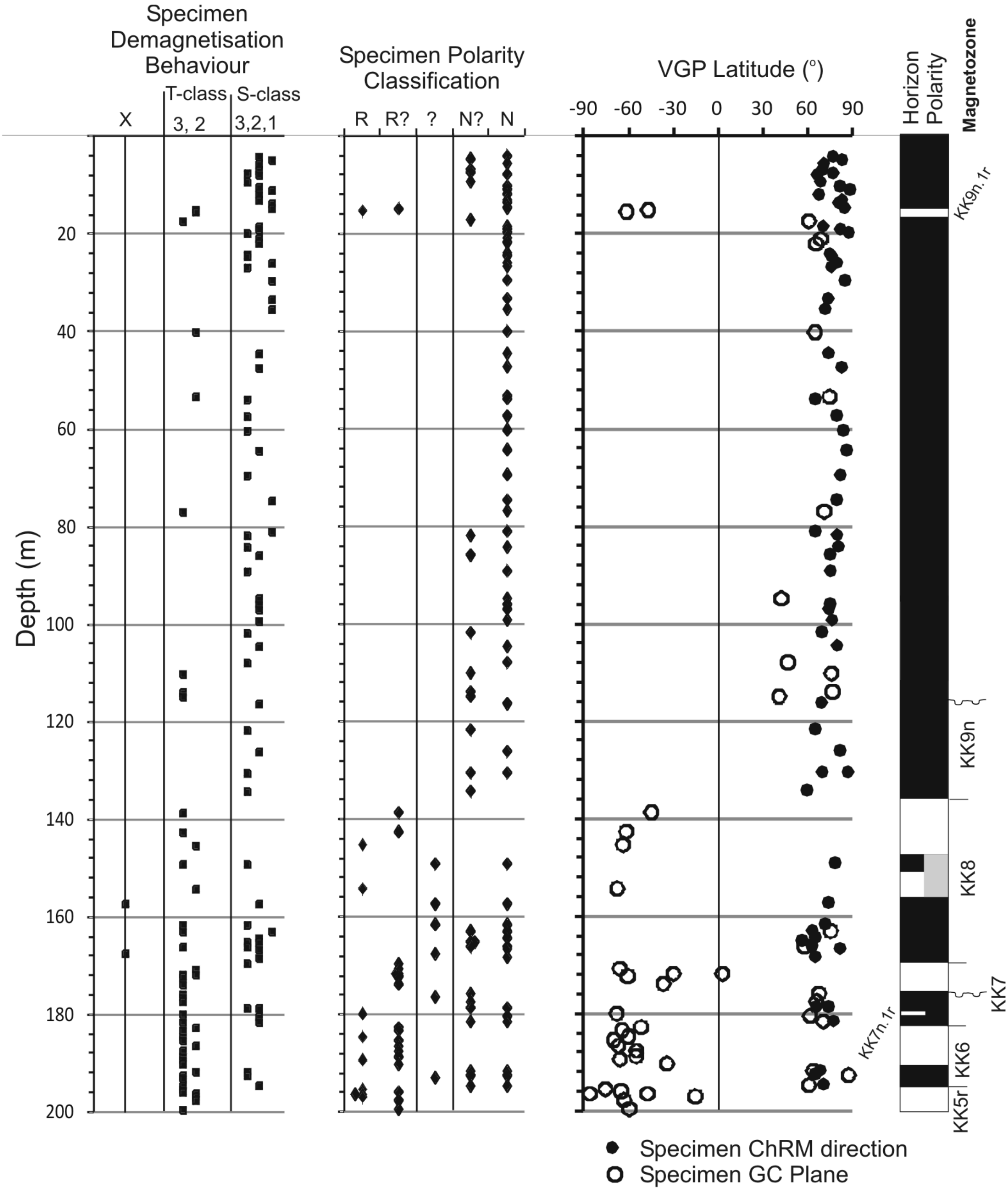

Figure 13. Summary Palaeomagnetic data from well 7830/3-u-1. Positions of probably significant hiatuses are shown. Details on caption to Fig. 12.

In core 7830/3-u-1, the dramatic increase in NRM intensity between depths 121.8 m and 116.45 m marks the transition into the thick cross-bedded channel-sandstone unit at around 116m. The coincidence of these changes suggests the units above 116 m correspond to a quite different stratigraphic unit, and probably marks a significant hiatus at this level. This is also shown by the overall thickness of the magnetic polarity zones which probably indicates a larger sedimentation rate in the units younger than the 116 m level compared to those below this level. Therefore broadly the magnetic and lithologic data suggest we have three major disconformity bound packages in this core, Unit F, Unit G up to ~116 m and the 3rd package above 116 m (Fig.11). Package 3 likely has a significantly larger sedimentation rate than the older units in this core, since it is dominated by normal polarity of a single major magnetochron.

The Re/Os dates from the two older cores suggest these are equivalent to an interval in the latest Ladinian (mid to late Longobardian), if comparison is made to the U/Pb dates from zircon-age dates through this interval (Fig. 14). However, the interval between 237.5 Ma and 235 Ma appears to be dominated by long normal polarity intervals (MT13 to UT1n), unlike the polarity data from cores 7831/2-u-2 and 7831/2-u-1 (Fig. 4). Consequently, the magnetostratigraphy suggests the two older cores probably correlate to the older interval around chrons MT11 to MT12 (Fig. 14).

A satisfactory match to the geomagnetic polarity timescale can be found for these two older cores through the interval between the upper part of MT11n into MT12r, with the uncored gap between these two cores probably representing the lower part of MT11r. Hounslow *et al.* (2008b) has correlated the upper-most part of the Botnehia Fm in central Spitsbergen to the upper-part of MT11n and lowest part of MT11r, which is the same interval seen in core 7831/2-u-2. The age interval MT11r to UT1r has not been identified in central Spitsbergen, but appears to be represented in core 7831/2-u-1 and the lower part of 7830/3-u-1. The proposed correlations for the upper part of 7830/3-u-1 are primarily constrained by the *Stolleyites* sp in 7830/3-u-1 which correlate it to the Tschermakfjellet Fm at Dalsnuten in central Spitsbergen (Fig. 14). This interpretation suggests that part of UT1n is missing at the hiatus at the base of package-2 in 7830/3-u-1. The magnetozone KK9n in 7830/3-u-1 may correspond entirely to the lower part of UT2n in the mid part of the Julian sub-stage (Fig. 14).

Overall this magnetostratigraphic match to the geomagnetic timescale is good apart from KK6n which is not represented in any other measured section near the Ladinian-Carnian boundary. Only the Carnian GSSP at Stoures has complete sample coverage through this interval, the Mayerling section has a sampling gap over MT13r (Fig. 14). Likewise sub-magnetozones KK1n.1r and KK8r.1n are not represented in other equivalent age sections. This may be a reflection of insufficient sampling density at other sections.

Using the proposed magnetostratigraphic correlations, it is clear there are significant offsets between the Re/Os dates and U/Pb dates, both of which can be directly tied to the magnetostratigraphy. Comparison of dates from different radiometric systems has remained problematic, with only recently recognised 1% differences in age between U/Pb and $^{40}Ar/^{39}Ar$ ages (Mundil *et al.* 2010), and differences between various pre-processing protocols. There does not appear to be a published assessment of intercalibration issues between Re/Os and U/Pb dates, and questions of how best to fully interrelate these differing geochronology tools are only just being asked (Selby et al. 2009).

The inferred age implied by this data conflict with the interpreted early Carnian palynomorphs in well 7831/2-u-1. At the Stoures GSSP in Italy the Canadensis Zone (marking the base of the Carnian) has the first occurrence of *Vallasporites ignacii*, *Patinasporites densus* and *Aulisporites* cf. *A. astigmosus*, together with *Duplicisporites verrucosus* and *Camerosporites secatus*, species which usefully allow some correlation with central and southern Europe. However, these probably do not allow a sufficiently detailed correlation of the GSSP to the Barents Sea succession. The rather poorly studied ammonoid succession through the late Ladinian interval in the Barents Sea region would probably need to be better integrated with a detailed palynology to help resolve finer scale correlation using pollen and spores through this interval.

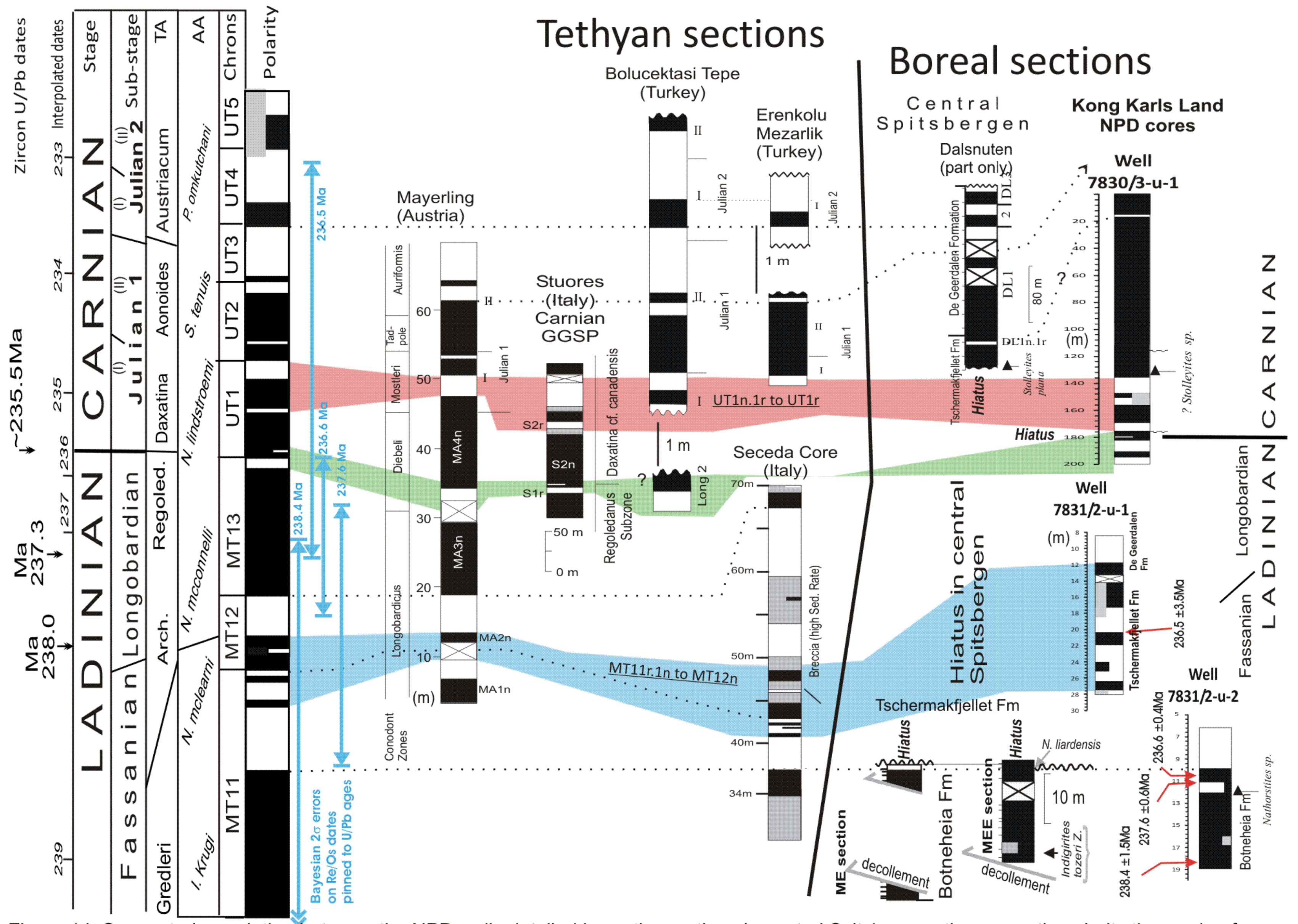

Figure 14. Suggested correlation between the NPD wells detailed here, the sections in central Spitsbergen the magnetic polarity timescale of Hounslow & Muttoni (2010), and other sections of this age with associated magnetostratigraphy. Correlations shown in coloured blocks and dotted lines. The Re/Os age ranges (in blue) and dates in Boreal sections shown in red (from Xu et al in press). TA= Tethyan standard ammonoid zones, AA= NE Asian ammonoid biozones.

Bibliography

Butler, R.F. 1992. *Paleomagnetism, magnetic domains to geologic terranes*, Blackwell, Oxford, 319pp. [at http://geography.lancs.ac.uk/cemp/resources/ Butler_book/contents.htm]

Dagys, A. S. & Weitschat, W. 1993. Correlation of the Boreal Triassic. *Mitteilungen Geologisch-Paläontologisches Institut Universität Hamburg*, **75**, 249-256.

Dagys A.S. & Konstantinov A.G. 1995. New zonation scheme of the Ladinian Stage for Northeastern Asia. *Stratigraphy and Geological Correlation **3***, 121-127.

Glørstad-Clark, E., Faleide, J.I., Lundschien, B.A. & Nystuen, J.P. 2010. Triassic seismic sequence stratigraphy and paleogeography of the western Barents Sea area. *Marine and Petroleum geology*, **27**, 1448-1475.

Hailwood, E.A & Ding, F. 1995. Palaeomagnetic re-orientation of cores and the magnetic fabric of hydrocarbon reservoirs. In: P. Turner & A. Turner (eds). *Palaeomagnetic applications in the hydrocarbon industry. Special Publication Geol. Soc. Lond.*, **98**: 245-258.

Hochuli, P. A., Colin, J. P. & Vigran, J. O. 1989. Triassic biostratigraphy of the Barents Sea area. *In*: Collinson, J. D. (ed), *Correlation in Hydrocarbon Exploration*, Norwegian Petroleum Society, Graham & Trotman, 131-153.

Hounslow, M.W., Hu, M., Mørk, A., Vigran, J.O., Weitschat, W. & Orchard M.J. 2007. Magneto-biostratigraphy of the lower part of the Kapp Toscana Group (Carnian), Vendomdalen, central Spitsbergen, arctic Norway. *Journal of the Geological Society, London,* **164**, 581-597.

Hounslow, M.W & Nawrocki, J. 2008a. Palaeomagnetism and magnetostratigraphy of the Permian and Triassic of Spitsbergen: a review of progress and challenges. *Polar Research*, **27**, 502–522.

Hounslow, M.W., Peters, C., Mørk, A., Weitschat, W. & Vigran, J.O. 2008b. Bio-magnetostratigraphy of the Vikinghøgda Formation, Svalbard (arctic Norway) and the geomagnetic polarity timescale for the Lower Triassic. *Geological Society of America Bulletin*, **120**, 1305-1325.

Hounslow, M.W., Hu, M., Mørk, A., Weitschat, W., Vigran, J.O., Karloukovski, V. & Orchard, M.J. 2008c. Intercalibration of Boreal and Tethyan timescales: the magneto-biostratigraphy of the Middle Triassic and the latest Early Triassic, central Spitsbergen (arctic Norway): *Polar Research*. **27**, 469-490.

Hounslow, M.W. & Muttoni, G. (2010). The Geomagnetic Polarity Timescale for the Triassic: linkage to stage boundary definitions. *In*: S. Lucas (ed.) *The Triassic Time scale*. Special Publication Geological Society. vol. **334**; 61-102.

Høy T. & Lundschien, B.A. 2011. Chapter 15 Triassic deltaic sequences in the northern Barents Sea. Geological Society, London, Memoirs, vol. **35**, p. 249-260.

Kent, J.T., Briden, J.C. and Mardia, K.V. 1983. Linear and planar structure in ordered mulivariate data as applied to progressive demagnetisation of palaeomagnetic remanance. *Geophys. Jour. Royal. astro. Soc*., **81**: 75-87

Krajewski K.P. 2008. The Botneheia Formation (Middle Triassic) in Edgeøya and Barentsøya, Svalbard: lithostratigraphy, facies, phosphogenesis, paleoenvironment. *Polish Polar Research,* **29**, 319–364.

Langereis, C. G.; Krijgsman, W; Muttoni, G.; Menning, M. 2010. Magnetostratigraphy concepts, definitions, and applications. Newsletters on Stratigraphy, 43, 207-233.

Mietto, P., Manfrin, S., Preto, N, Rigo, M. Roghi, G., Furin, S., Gianolla, P., Posenato, R., Muttoni, G., Nicora, A., Buratti, N., Cirilli, S., Spötl, C, Ramezani, J., and Bowring, S.A. 2012. The Global Boundary Stratotype Section and Point (GSSP) of the Carnian Stage (Late Triassic) at Prati Di Stuores/Stuores Wiesen Section (Southern Alps, NE Italy). *Episodes*, **35**, 414-430.

Mørk, A., Knarud, R. & Worsley, D. 1982: Depositional and diagenetic environments of the

Triassic and Lower Jurassic succession of Svalbard. *In*: Embry, A.F. & Balkwill, H. R. (eds), *Arctic Geology and Geophysics*, Canadian Society of Petroleum Geologists, Memoir **8**, 371-398.

Mørk, A., Dallmann, W.K., Dypvik, H., Johannessen, E.P., Larssen, G.B., Nagy, J., Nøttvedt, A., Olaussen, S., Pchelina, T.M., Worsley, D., 1999. Mesozoic lithostratigraphy. In: Dallmann, W.K. (Ed.), Lithostratigraphic lexicon of Svalbard. Review and recommendations for nomenclature use. : Upper Palaeozoic to Quaternary bedrock. Norsk Polarinstitutt, Tromsø, pp. 127–214.

Mundil R., Palfy, J., Renne, P.R. Brack, P. 2010. The Triassic timescale: new constraints and a review of geochronological data. *In*: S. Lucas (ed.) *The Triassic Time scale*. Special Publication Geological Society. **334**, 41-61.

Opdyke, N.D & Channel, J.E.T. 1996. *Magnetic Stratigraphy*, Acedemic press, London, 346pp.

Rolph, T.C, Shaw, J., Harper, T.R. & Hagan, J.T. 1995. Viscous remanent magnetisation: a tool for orientation of drill cores. In: P. Turner & A. Turner (eds). *Palaeomagnetic applications in the hydrocarbon industry. Special Publication Geol. Soc. Lond.*, **98**: 239-244.

Riis, F., Lundschien, B.A., Høy, T. Mørk, A. & Mørk, M.B. 2008. Evolution of the Triassic shelf in the northern Barents Sea region. *Polar Research* **27**, 318-338.

Selby, D. Mutterlose, J. Condon, D.J. 2009. U–Pb and Re–Os geochronology of the Aptian/Albian and Cenomanian/Turonian stage boundaries: Implications for timescale calibration, osmium isotope seawater composition and Re–Os systematics in organic-rich sediments. *Chemical Geology*, **265**, 394–409.

Torsvik T.H. & Cocks L.R.M. 2005. Norway in space and time: A Centennial cavalcade. *Norwegian Journal of Geology* **85**, 73-86.

Vigran, J.O., Mangerud, G., Mørk, A., Bugge, T. & Weitschat, W. 1998. Biostratigraphy and sequence stratigraphy of the Lower and Middle Triassic deposits from the Svalis Dome, Central Barents Sea, Norway. *Palynology*, **22**, 89-141.

Vigran J.O., Mørk A. & Worsley D inpress. Palynology and geology of the Triassic succession of Svalbard. *NGU Bulletin*.

Worsley D. Johansen, R. & Kristensen, S.E. 1988. The Mesozoic and Cenozoic succession of Tromsøflaket. In Dalland et al. (eds). *A lithostratigraphy scheme for the Mesozoic and Cenozoic succession offshore mid and northern Norway*. Norwegian Petroleum Directorate Bulletin **4**, 42-65. Stavanger: NPD.

Xu G. Hannah, J.L. Stein, H.J. Mørk, A., Bingen, B., Schutt, D., Lundschien, B.A. in press. Cause of Upper Triassic climate crisis revealed by Re-Os geochemistry of Boreal black Shales. *Palaeogeog. Palaeoclim. Palaecol*.

Appendix 1:

A1. Introduction to magnetostratigraphy and palaeomagnetism

The purpose here is to introduce some elements of palaeomagnetism which are relevant to the objectives of this work, and are necessary for understanding the detailed analysis presented here. More thorough introductions to the various sub-topics can be found in Butler (1992), and more details, specifically focusing on magnetostratigraphy can be found in Langereis *et al.* (2010) and Opdyke & Channel (1996). A glossary of terms and concepts in given in Appendix 2.

A1.1 The Earth's magnetic field

The magnetic field of the Earth is generated within the core due to a magneto -dynamo effect. The form of this magnetic field at the Earth's surface is such that it can be ascribed to a two component system. The first, the dipole component (i.e. the **geocentric axial dipole**) is the main component of the magnetic field. This can be equated to a bar magnet with a fixed north and south pole, which are effectively located over the Geographic North and South Pole respectively. The inclination (see *Appendix 2*) of this dipole field is systematically related to the latitude of observation by $\tan(I) = 2\tan \varphi$ (I= inclination, φ= latitude). This relationship is such that near the present day North Pole the magnetic field is steeply dipping downwards, and near the equator the field is shallowly dipping and directed northwards. This equation is the fundamental basis of many palaeomagnetic studies, since it can predicted site palaeolatitude from inclination.

The second element of the magnetic field is the non-dipole component. This is a subsidiary magnetic field which can be described by a complex set of Fourier harmonics. This non-dipole field varies in intensity and direction through time (the change is called **secular variation**) and gives rise to the current displacement of the magnetic north pole into the region of Arctic Canada.

If the direction of the magnetic field could be averaged over a sufficiently long period of time (~10,000 yrs), the secular variation would be averaged out and the mean direction would correspond closely to the expected position of the geocentric axial dipole field (i.e. north geographic pole). Conversely, if the magnetic field direction is recorded over a short period of time, the recorded direction may be displaced from the geocentric axial dipole position due to this non-dipole field component.

A1.2 Magnetostratigraphy

The geocentric axial dipole component of the magnetic field has periodically reversed through geologic time, flipping between the current state (**normal polarity**) and the opposite state (magnetic field north pole over South Geographic Pole, called **reversed polarity).** The last polarity change occurred 0.78 million years ago, and since that time the current interval of normal polarity magnetic field is referred to as the **Brunhes**. The rate of field reversal has changed through time, with intervals of constant polarity in the Late Cretaceous (normal polarity) and the Late Carboniferous to Mid Permian (reverse polarity). Magnetozone duration ranges from several 10's of million years to ~30,000 years. The time it takes to switch magnetic field polarity is of the order of 1,000 to 8,000 years, shorter in duration than a single Milankovitch precession cycle.

A1.3 Recording of the magnetic field

When sediments are formed they record the direction of the magnetic field, because they contain small amounts of magnetic minerals (i.e. primarily magnetite. Fe_3O_4), which are forced to orientate into the direction of the ambient magnetic field. Palaeomagnetists can then come along at a later date, collect a piece of the sediment and measure the direction and magnitude of this weak, preserved **remanent magnetisation** (remanent magnetisation is a vector). The current consensus is that compaction and the activity of burrowing organisms can impart a **post-Depositional Remanent Magnetisation** (pDRM) in the direction of the ambient magnetic field, due to re-adjustment in early sediment fabrics. This form of remanent magnetisation is commonly preserved, and is possibly acquired over a period of a few 10s to 100s of years during very early burial.

Sediments subjected to time, diagenetic processes, burial and heating can have this pDRM partially **overprinted** by later remanence directions, perhaps acquired in differently oriented magnetic fields. Time is an important part of the magnetisation process, since remanent magnetisations to some extent will decay naturally (i.e. through **viscous decay**), due to the physics of the magnetic recording particles (Butler, 1992). For exactly the same reason, music recorded on magnetic tape gradually looses its quality with time. Equally, magnetic materials can slowly acquire any new field direction by a **viscous magnetisation** process (this remanence is called a Viscous Remanent Magnetisation, or **VRM**). The rate at which this occurs is strongly dependent upon the grain size, type of magnetic mineral and burial temperature (**multidomain** magnetite is particularly prone to acquiring VRM). Where enhanced temperature is important, the VRM acquired is often called a Thermo-Viscous Remanent Magnetisation (**TVRM**). This type of magnetisation acquisition behaviour is thought to be one of the major processes responsible for the acquisition of overprint magnetisations in reservoir rocks. It is this TVRM component which is commonly used for re-orienting core material using palaeomagnetic measurements (Rolph et al., 1995; Hailwood and Ding, 1995). In this study we have attempted to recover the specimen TVRM directions, in addition to the Triassic directions in order to re-orient the samples back into their *in situ* positions.

Diagenetic processes can be effective in modifying the Fe-bearing magnetic minerals, which carry the original recorded magnetic field signal. Under reducing conditions in sediments the major diagenetic pathway for magnetic minerals is their dissolution, so that we would expect < 5 % of the originally deposited magnetic oxides to be preserved, if buried to any significant depth. Under some situations diagenesis can produce new magnetic minerals, such as magnetic sulphides (greigite and some form of pyrrhotite) or haematite, which may acquire the magnetic field direction on growth. These new growing minerals can acquire a Chemical Remanent Magnetisation (**CRM**). In Permo-Triassic sequences, haematite authigenesis is significant since much of the haematite (which gives rise to the sometimes red colouration) present in the sequences is produced during diagenesis. Many studies have shown the recovery of good magnetostratigraphic signals from red bed-successions, whose magnetic signal is mostly retained due to the coarser grained haematite particles, which may in part be detrital in origin. Much of the finer grained haematite which contributes to the red-body colour, and is often seen to be a late diagenetic product and is mostly not significant for palaeomagnetic and magnetostratigraphic studies (since its too fine-grained).

The major part of palaeomagnetic work is to remove the later magnetic overprints by the process of **demagnetisation** (also called 'magnetic cleaning') and to isolate the originally recorded magnetic field direction. This process also allows palaeomagnetic studies to isolate and analyse the various magnetic field components which may be recorded by a specimen.

A1.4 Types of magnetic minerals

In sediments there are several types of minerals that can act as recorders of the magnetic field (*Table A1*). Each of these minerals can retain a remanent magnetisation. Magnetite and its magnetically similar titanomagnetite group minerals (e.g. Fe_3O_4 to Fe_2TiO_4 solid solution) are often considered the most important, because these are strongly magnetic and abundant in igneous and metamorphic source rocks.

Within each mineral group, a number of factors influence the magnetic properties of these minerals. These various properties can be useful in: a) distinguishing which mineral is carrying the remanent magnetisation, and b) allow the separation and isolation (during demagnetisation) of the recorded magnetic field information carried by different minerals.

Temperature: Each magnetic mineral has a specific upper temperature above which it can no longer retain its remanent magnetisation. This temperature is its **Curie temperature**, and can be diagnostic of the mineral carrying the remanence.

Grain size: The size of the magnetic particle is a fundamental control on its magnetic behaviour. This is primarily expressed through the grain's **coercivity**, which can be thought of as the degree of difficulty with which the direction of the intrinsic remanent magnetisation can be reset, without physically rotating the grain. Generally within any mineral group, the larger the grain size the smaller the coercivity (i.e. more easily reset). Unfortunately, grain-size - coercivity relationships are not quite as simple as this, and palaeomagnetic studies often talk about **multidomain** (largest grains) and **single domain** grains (mostly grains ~0.1μm in size), when describing magnetic grain behaviour. Single domain grains are the most resistant to resetting by later events (i.e. TVRM), so it is the magnetic field direction recorded by these grains that demagnetisation is trying to isolate.

In addition to differences in grain size controlling coercivity, different minerals can have markedly different coercivity. For example, magnetite and pyrrhotite have a relatively low coercivity, compared to haematite whose coercivity is approximately one order of magnitude larger than magnetite of the same grain size.

Mineral Group	Composition	Typical origin	Magnetic characteristic	Curie temperature
Magnetite	Fe_3O_4	Detrital	low coercivity	580 °C
Haematite	Fe_2O_3	Detrital/ Diagenetic	high coercivity	710 °C
Pyrrhotite	Fe_7S_8-Fe_9S_{10}	Diagenetic	low coercivity	~320 °C
Greigite	Fe_3S_4	Diagenetic	moderate coercivity	~320 °C
Goethite	γFeOOH	Weathering	Very high coercivity	~120 °C

Table A1. The main groups of magnetic minerals which are significant in carrying remanent magnetisation in sediments and some of their properties.

A1.5 Introduction to demagnetisation procedures

The remanent magnetisation of any specimen, once it has been collected and first measured is called the Natural Remanent Magnetisation (NRM). This NRM may be composed of several components, namely the **Characteristic Remanent Magnetisation** component (**ChRM),** acquired at (or close to) the time of deposition, and any later **overprints** (i.e. TVRM or CRM) which may have been acquired after this time. It is the purpose of demagnetisation to remove these overprints, so the ChRM direction can be defined.

There are various methods of demagnetising rocks; the two most commonly used include alternating field (AF) methods and thermal methods. These are summarised in *Table A2* and outlined below.

Alternating Field (AF) Demagnetisation: The sample is randomly tumbled in an alternating magnetic field which is slowly reduced in intensity from a peak value to zero (the sample and alternating field are inside a magnetic shield which reduces the ambient Earth's magnetic field to near zero). This procedure randomises the magnetic moments of grains with coercivities up to the value of the applied field. Progressively larger peak fields are applied to remove magnetic components due to grains with larger coercivities. Typically, AF magnetic fields in increments of 5 or 10 mT are used. Between each demagnetisation step, the remanent magnetisation of the specimen is measured, which allows analysis of the behaviour of the NRM as it is slowly stripped away.

Thermal Demagnetisation: Samples are heated to a specific temperature and then allowed to cool to room-temperature in a zero magnetic field. Heating a sample in this way randomises the magnetisation of specific types of magnetic grains. The grains which are randomised at this temperature are those whose '**blocking temperature**' is less than this temperature. Thermal demagnetisation is thought to be particularly effective in removing magnetisation due to thermo-viscous overprints, perhaps caused by a long period of burial at elevated temperatures. It is also the only way to demagnetise remanence carried by haematite or goethite, because routine AF demagnetisation equipment cannot achieve large enough magnetic fields to exceed the coercivity of the minerals.

Low temperature demagnetisation: Samples are cooled to liquid nitrogen temperature (-196 ^{o}C) and subsequently warmed back to room temperature in a zero magnetic field. This removes the magnetisation due to multi-domain (i.e. grains > ~ 10 µm) magnetite grains only. This method has not been used in this study.

Method	Equipment Used	Procedure	Minerals effective on	Treatment Range
Alternating Field Demagnetisation (AF)	Alternating magnetic field applied to specimen in zero direct field	AF ramped to peak field, and slowly reduced	Magnetites, Magnetic sulphides	0 to 100 mT peak AF fields
Thermal Demagnetisation	Oven inside a zero magnetic field	Specimen heated to peak temperature for ~20 minutes, and cooled in zero magnetic field	Magnetite, Haematite, Magnetic sulphides, Goethite	50- 720 ^{o}C

Table A2. Main types of demagnetisation method used in this study and their 'characteristics'.

A1.6 Magnetic measurement equipment

During the demagnetisation procedures the remanent magnetisation of all specimens was measured using a CCL GM400 3-axis cryogenic magnetometer. This has a sensitivity limit of ~0.002 mA/m, which is more than adequate for the specimens in this study, which have typical NRM values of 0.5-20.0 mA/m. Magnetisation measurements comprise 4-16 (depending upon intensity) individual determinations, from which the variance is determined. The thermal demagnetiser used was a Magnetic Measurements MMTD1, which sits inside a field cancellation coil, and has additional field cancellation through an external power supply to the TRM coil. Alternating field demagnetisation was performed with a Molspin reversing, tumbling demagnetiser. Specimens in intermediate stages of demagnetisation were stored in mu-metal, zero field boxes to reduce the likelihood of acquisition of VRM in the laboratory.

Low field magnetic susceptibility was measured on a Bartington MS2 meter. Magnetic susceptibility of specimens was measured after each thermal demagnetisation step to monitor changes in magnetic mineralogy caused by the heating process.

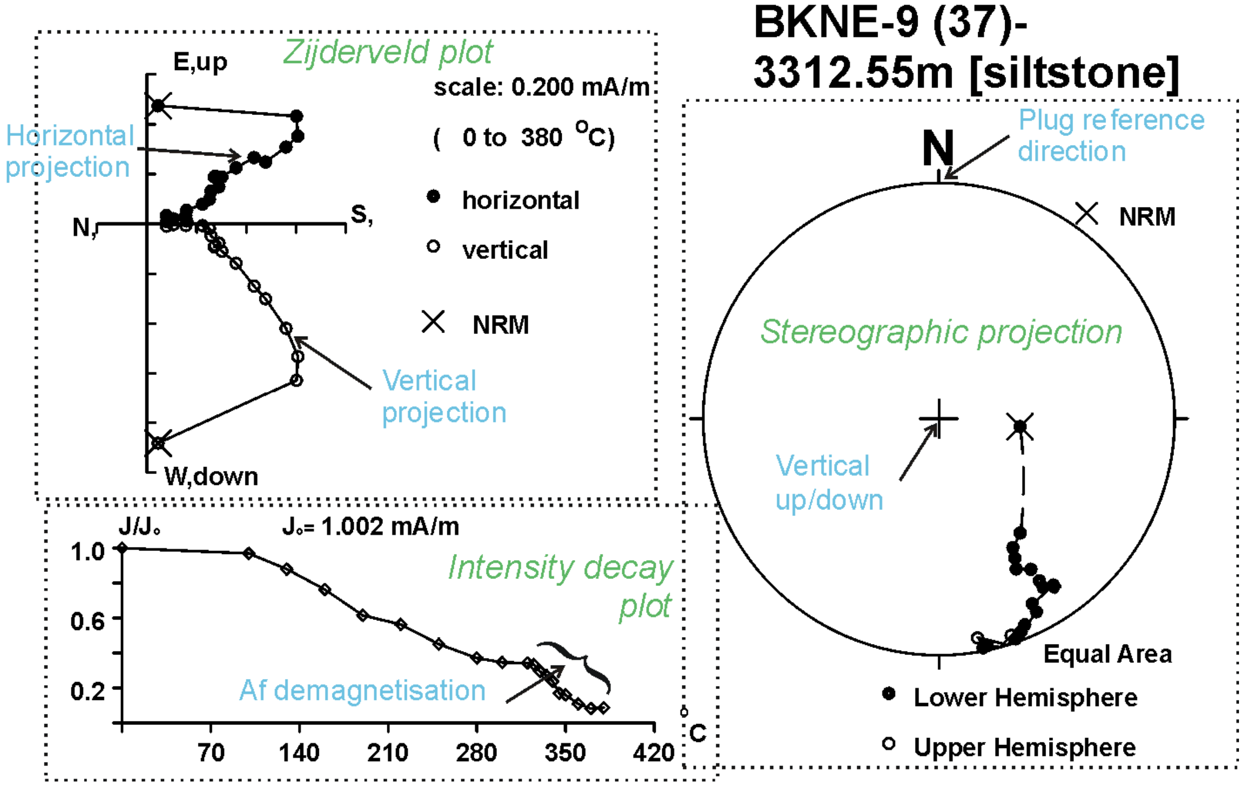

Figure A1 Example of the type of diagram indicating the style of data presentation used for specimen demagnetisation data described in this report. See text for details (sample shown is illustrative and not from this study).

A1.7 Data presentation

Palaeomagnetic data for specimens is displayed in three ways, using diagrams like *Figure A1*. Graphs in these demagnetisation figures are composed of: a) Zijderveld diagram, b) Stereographic projection and c) a J/J_0 plot (intensity decay plot). These graphs display the specimen demagnetisation data after it has been rotated back into core coordinates. Specimens which come from an unoriented core, are oriented with reference to the sample fiducial (F) rather than North, which is not known (Zijderveld and stereographic projection diagrams for unoriented core actually indicate North (N) which for presentation purposes is the same as the fiducial direction (F)).

a) The Zijderveld diagram presents both the directional and magnitude information of the remanence vector as it is demagnetised. In these diagrams, the distance from the origin (crossing point of axes) corresponds to the magnitude of the remanence vector. Equal intensity scale between axis ticks are used on each of the 4 axes, and are shown on the diagram in mA/m. As a result of demagnetisation, the NRM vector generally plots furthest from the origin, and the last demagnetisation step nearest the origin.

The remanence vector directional information, which is 3-dimensional, is reduced to the 2-dimensions of the paper, by projecting the position of the vector onto 2 orthogonal planes, a horizontal one and a vertical one (indicated on diagram with filled and open symbols). An axis common to both projection planes is shared in the diagram (e.g. E,up; W,down in *Fig. A1*). The vertical projection planes are either East-West or North-South oriented, depending upon which projection is suitably oriented for displaying the maximum spread in data points. The vertical plane in *Figure A1* is aligned N-S.

The most important point to appreciate is that the removal of a single component of magnetisation results in straight lines (one for each projection) on the Zijderveld diagram connecting demagnetisation steps. Specimens which have curved segments on Zijderveld diagrams do so because the coercivity spectra (or blocking temperature spectra) of the ChRM and overprint magnetisations overlap (see Appendix).

If demagnetisation data is noisy, the Zijderveld diagram may not be the best means for visually examining the data. Stereographic projections often produce a clearer picture of the specimen's behaviour. This is because there is no clear simple means of plotting the error-envelope (from the measured variance) on each magnetisation measurement on the Zijderveld diagram.

b) Stereographic Projection: The direction of the remanence vector is plotted on an equal area stereographic projection which displays only the directional information, with negative inclination (i.e. potentially reversed polarity) plotted as open circles and positive inclinations (potentially normal polarity) with filled circles. The core axis is in the vertical position, in these diagrams. The horizontal projection plane of the Zijderveld diagram is comparable to the stereographic projection. For example *Figure A1,* shows measurement points plotting in the SE quadrant on the stereonet and the SE quadrant of the horizontal projection of the Zijderveld diagram (filled circles on Zijderveld diagram).

c) J/J_0 plot: This displays the remanence intensity decay with either AF demagnetisation field, or temperature. The intensity is normalised to the initial NRM intensity (i.e. NRM intensity =1.0), and the NRM intensity (J_o) in mA/m (10^{-3} A/m) is shown just above the diagram (*Fig. A1*). The intensity will generally decay the larger the demagnetisation value used, although when the specimen contains two opposite directed magnetisation and one is removed, the resulting intensity may rise. AF demagnetisation steps are added to the end of the thermal demagnetisation steps, and are displayed as the closely spaced points like in *Figure A1*.

Appendix 2: Glossary of palaeomagnetic terms

α95 (*Alpha 95*). This is a measure of 3-dimensional angular dispersion (in degrees), commonly used in palaeomagnetism, which is derived from *Fisher Statistics.* It is the angular radius of a cone about the mean direction, in which the true population mean is found. There is 95% probability that the population mean lies within this cone, about the mean direction.

Apparent polar wander path (APW): Due to the motion of the continents through continental drift (and plate tectonics) the apparent position of the geographic north pole will change with time. The path mapped out by the motion of this pole is the apparent polar wander path. A point on this path at any point in earth’s history can be determined by measuring a virtual geomagnetic pole for a set of rocks, which cover sufficient time to average the secular variation of the geomagnetic field.

Blocking Temperature. This is the transition temperature between when a grain is superparamagnetic and single domain. In essence, for each magnetic particle there is a specific temperature, (below the Curie temperature) above which it can no longer retain its remanent magnetisation- i.e. its blocking temperature. The blocking temperature is strongly grain-size dependent, with very small *single domain* particles having lower blocking temperatures than slightly larger single domain grains.

Coercivity (or coercive force) is the ease with which the remanent magnetisation of a grain or specimen can be reset into a new direction (i.e. *magnetised*, or demagnetised in this direction) by an applied magnetic field. This is measured in terms of the magnetic field (in MilliTesla, mT) required to do this. The coercivity of a mineral is strongly related to its grain size, such that smaller grains (above the superparamagnetic size threshold) need a larger magnetic field than bigger grains in order to ‘demagnetise’ them.

Coercivity Spectra A specimens remanent magnetic properties are due to a mineral (perhaps 2 or more minerals), of various grain sizes. Consequently, the magnetic field (coercive force) required to ‘demagnetise’ these various sized magnetic particles will also vary over a range of values. Consequently it is common to talk about coercivity spectra, which can be roughly equated with a spectrum of ‘magnetic grain sizes’ present in a sample.

ChRM (*Characteristic Remanent Magnetisation*). This term is used to described what a palaeomagnetist interprets may be a specimens remanent magnetisation produced when the rock was formed. Whether this was a *pDRM, CRM* or a *VRM* depends on other data which is not attainable from demagnetisation data of a single specimen. The ChRM is generally (but not always) interpreted to be the last component (i.e. linear segment going through origin of the Zijderveld plot) recoverable from the demagnetisation data.

CRM (*Chemical Remanent Magnetisation*). The type of remanent magnetisation acquired when magnetic grains capable of carrying a remanence nucleate from fluids, or are formed from other minerals (such as during diagenesis). Such grains need to grow through a critical size (below which they are superparamagnetic), called its blocking volume.

Declination. The angle between north and the horizontal projection of the magnetisation vector. i.e. 0^o == North directed; 180^o == South directed; 90^o == East Directed; 270^o == West directed. In specimens from unoriented core material the declination is measured from the sample fiducial direction.

Diamagnetic. Pure materials and minerals which acquire an induced magnetisation in the *opposite direction* to an applied magnetic field, are diamagnetic. Such phases have a small negative magnetic susceptibility. When the magnetic field is removed, they retain NO remanent magnetisation. Common examples of diamagnetic minerals are non-Fe/Mn bearing silicates (e.g. quartz, feldspar) and carbonates containing no Fe/Mn (e.g. calcite, dolomite)

Drilling- Induced Remanent Magnetisation (DIRM): This enigmatic type of remanence can be common in rocks collected from commercial coring operation, or sub-coring from such cores, although it is not restricted to such material, but is also often not present. Basically the rock specimens acquire a magnetisation in the direction (either up or down) of the coring axis, due to the stray magnetic field generated by the drill bit or drill string. The magnetisation process by which this occurs is poorly understood, and may be produced from a variety of origins. Perhaps the most likely is a stress-release related mechanism (properties of magnetic grains can be related to their stress state). A DIRM may be associated with the main coring, or plugging of the specimens from the core using the 1" diamond tipped drill bits in the core stores. This 'plugging remanence' may also be associated with a stress release mechanism, although it is normal to use non-magnetic drill bits, which alleviate, but perhaps not eliminate this enigmatic 'plugging remanence'.

Ferrimagnetic/ Ferromagnetic. Minerals which can acquire a permanent magnetisation, which can be retained in the absence of an applied magnetic field (e.g. magnetite). There are a number of sub-groups of magnetic behaviour within this broad grouping. These minerals generally have a large magnetic susceptibility compared to paramagnetic and diamagnetic materials. Common examples are titanomagnetite, haematite (canted antiferromagnetic), pyrrhotite & greigite (ferrimagnetic).

Fiducial: A reference direction and mark on the specimen, which is used relate the specimen orientation to horizontal and geographic north. In the case of unoriented core, this is a mark pointing up-core, along the axis of the core.

Fisher Statistics: The commonly used statistical method of averaging 3-dimensional vectors (Butler, 1992). Three- dimensional equivalent of the 1-dimensional normal statistics.

Geocentric Axial Dipole: A model of the Earth's magnetic field which excludes the non-dipole magnetic field components. In this model the magnetic north and south pole are located over the spin axes of the Earth, and the relationship between latitude (γ) and inclination (I) is described by Tan (I) = 2Tan (γ).

Inclination. The angle between horizontal and the magnetisation vector, such that a downwards directed vector has positive inclination and an upwards directed vector has negative inclination.

Induced Magnetisation (See magnetisation and magnetic susceptibility).

Magnetic Susceptibility . When a material is exposed to a magnetic field (H) it acquires an *induced magnetisation*, J_i, such that $J_i=\chi H$, where χ is the magnetic susceptibility. All materials posses a magnetic susceptibility, including *diamagnetic*, *paramagnetic* and *ferrimagnetic* materials, but because ferrimagnetic materials (e.g. magnetite) have magnetic susceptibility several orders of magnitude larger than paramagnetic materials, it is common to think of magnetic susceptibility as a measure of the 'concentration of magnetic materials'. Volume specific magnetic susceptibility (shown as k) has no units in SI (i.e. J_i and H have same units), but when expressed on a mass specific basis its units are $m^3\ Kg^{-1}$.

Magnetisation. The magnetisation of a material is the net magnetic moment per unit volume. There are two types of magnetisation, *induced and remanent magnetisation*. The *induced magnetisation* is associated with the magnetic susceptibility, and is ONLY found and measured when materials are in a magnetic field. Remanent magnetisation is a 'permanent magnetisation' and is that which enables rocks to record the direction of magnetic fields at their time of formation.

Magnetozone: A stratigraphic interval in a rock section or core defined by sampling, of either reversed or normal polarity. A magnetozone may be all normal, all reverse or consist of a normal-reverse couplet. When the polarity zones represent chronostratigraphic time intervals they are called magnetochrons (or chrons for short).

Multidomain: (see single domain).

NRM (*Natural Remanent Magnetisation*). The remanent magnetisation of a rock, as it is first measured, prior to laboratory treatment. This may be composed of one of more magnetisation components, perhaps acquired in different times and under different processes.

Paramagnetic. Minerals that acquire an induced magnetisation in the direction of an applied magnetic field are paramagnetic. These also have a positive magnetic susceptibility, generally related to the Fe and Mn-content of the phase. When the magnetic field is removed, they retain NO remanent magnetisation. Common examples of these are Fe or Mn-bearing silicates and carbonates.

pDRM (post Depositional Remanent Magnetisation). The remanent magnetisation acquired close to the time of deposition due to re-organisation of sediment fabric perhaps through activity of burrowing organisms and early sediment compaction.

Plugging Remanence: A spurious magnetisation aligned along the axis of the core plug (see DIRM)

Remanent Magnetisation. The magnetisation of a specimen which is permanent, and can be likened to that of a bar magnet, having a north and a south pole (i.e. has vector properties). The remanent magnetisation vector is expressed in terms of *declination*, *inclination* and magnitude. When this magnitude is expressed on a volume specific basis its units are A/m (or mA/m = 10^{-3} A/m), but on a mass specific basis (to allow for changes in density) its units are Am^2 Kg^{-1} (magnetic moment per Kg).

Single Domain: In ferromagnetic particles, as a result of the energy-charge configuration, individual magnetic particles may be internally sub-divided into *domains.* These domains each have different directional alignment of the magnetisation, and contribute to the overall magnetisation of the whole grain. When the particles are small (<~0.1µm for spherical magnetite) these particles consist of only 1 domain, and are called *single domain* grains. When magnetite particles are larger than 10µm they consist of lots of domains. This type of particle is called a *multidomain* grain. Single domain and multidomain grains of a specific mineral each have characteristic magnetic properties. Unfortunately, natural magnetic particles also come in different shapes, and are intergrown or subdivided by other (perhaps non-magnetic) sub-regions, so that 'magnetic grain size' (i.e. single domain or multidomain behaviour) may not correspond to the physical size of a magnetic grain. For example, a detrital magnetite particle of say 30µm may be sub-divided internally (by exsolution of other minerals, etc.) so that this single detrital grain may possess single domain **and** multidomain behaviour, or perhaps only single domain behaviour.

Susceptibility (see magnetic susceptibility).

Superparamagnetic. Particles which display ferromagnetic/ferrimagnetic behaviour can also be superparamagnetic when these grains are very small. This means that they can retain a remanent magnetisation, but only for a very short period of time. The time over which this retention occurs is grain size dependent (superparamagnetic magnetite grains are <~0.02µm), perhaps from 10^{-10}s to a convenient value of 100s considered by Butler (1992). Such superparamagnetic grains loose the retained remanence due to thermal agitation of the atoms. In palaeomagnetic practice such grains are similar to paramagnetic grains, and do not carry a palaeomagnetic remanence.

Thermo-Viscous Remanent Magnetisation (TVRM). At elevated temperatures, below the Curie temperature, the rate of acquisition of VRM is accelerated, compared to VRM acquisition at lower temperatures. Since most reservoirs are buried at elevated temperatures of ~100^{o}C, these will acquire a thermoviscous remanence in the average direction of the geomagnetic field since the start of the Brunhes (~0.7 Ma ago) normal magnetic polarity chron.

VGP Latitude: This is a robust measure of the specimen polarity, which uses both the ChRM declination and inclination (if rotated into geographic coordinates using the TVRM). This is the latitude the specimen ChRM direction would correspond to if the site/core mean direction were rotated to correspond to the geographic north pole.

Virtual Geomagnetic Pole (VGP). The apparent position (in latitude and longitude) of the time averaged north magnetic field (i.e. the north geographic pole) for a set of samples. This assumes the geomagnetic field is approximated by a geocentric axial dipole. For progressively older times from the Holocene, this direction will deviate progressively from the north geographic pole due to continental drift.

Viscous Decay: The acquisition of VRM can be reversed, if the specimen is left in a zero magnetic field for long enough. Putting a specimen in such a zero field space allows any VRM component to decay to some extent. The natural decay of any acquired VRM is utilised by placing samples in a mu-metal box, which has a near zero magnetic field. This reduces any VRM which may have been acquired during laboratory handling.

VRM (*Viscous Remanent Magnetisation*). Remanent magnetisation, which is acquired by magnetic grains when exposed to a weak magnetic field, over a period of time. This may 'overprint' the original magnetisation of the rock acquired at the time of formation. The magnitude of VRM acquisition can be described by S.log(t), where S= the viscosity coefficient and t is time. S is related to the grain volume, whether it is a multidomain or single domain grain and the temperature (Butler, 1992). Generally in rocks, multidomain grains acquire VRM much faster than single domain grains.

Zijderveld diagram. A standard method of displaying the remanent magnetisation of a specimen as it is progressively demagnetised (also called vector end point, vector component, or orthogonal projection diagrams). See section A1.7 for a more detailed description. The use of Zijderveld diagrams in interpreting the demagnetisation behaviour of specimens is important for reliable palaeomagnetic studies. This is because, such diagrams allow the user to evaluate when a magnetic component is being removed, and if it may overlap with another magnetic component in the specimen. In natural specimens, as well as different degrees of overlap of overprint and ChRM, measurement errors are also added to the data, so that measured points on a straight line segment may appear to jump from side to side. This is more noticeable near the origin of Zijderveld plots. When data does become noisy the data displayed on the stereographic projection will be more useful for interpretation. Also, programs like LINEFIND can 'look through' the statistical noise in the data to isolate the correct ChRM.